Available online at www.sciencedirect.com
SCIENCE DIRECT
Tectonophysics 420 (2006) 49–73
TECTONOPHYSICS
www.elsevier.com/locate/tecto

Seismic velocity model of the crust and uppermost mantle around the Mirnyi kimberlite field in Siberia

V.D. Suvorov [a], E.A. Melnik [b], H. Thybo [b,*], E. Perchuć [c], B.S. Parasotka [d]

[a] Institute of Geophysics SB RAS, 3, Academician Koptyug Pr., Novosibirsk, 630090, Russia
[b] Geological Institute, University of Copenhagen, Øster Voldgade 10, DK-1350 Copenhagen K, Denmark
[c] Institute of Geophysics, Polish Academy of Sciences, ul. Ksiecia Janusza 64, 01-450 Warsaw, Poland
[d] Almazy Rossii-Sakha Ltd., Botuobya Enterprise, ul. Lenina 44b, Mirny, 678170, Russia

Received 29 January 2005; received in revised form 13 October 2005; accepted 4 January 2006
Available online 11 April 2006

Abstract

We present the first detailed seismic velocity models of the crust and uppermost mantle around the Mirnyi kimberlite field in Yakutia, Siberia. We have digitized vintage seismograms that were acquired in 1981 and 1983 by use of Taiga analogue seismographs along two perpendicular seismic profiles. The 370-km long, northwest striking profile I across the kimberlite pipe was covered by 41 seismographs, which recorded seismic signals from 21 chemical shots along the line, including one off-end shot. The perpendicular, 340-km long profile II across profile I ca. 30 km to the south of the Mirnyi kimberlite field was covered by 45 seismographs, which recorded seismic signals from 22 chemical shots, including four off-end shots. Each shot involved detonation of between 1.5 and 6.0 tons of TNT, distributed in individual charges of 100–200 kg in shallow water (<2 m deep). The data is of high quality with high signal/noise ratio to the farthest offsets. We present the results from two-dimensional ray tracing, forward modelling.

Both velocity models show normal cratonic structure of the ca. 45-km-thick crust with only slight undulation of the Moho. However, relatively small seismic velocity is detected to 25-km depth in a ca. 60-km wide zone around the kimberlite pipe, surrounded by elevated velocity (>6.3 km/s) in the upper crust. The lower crust has a relatively constant velocity of 6.8–6.9 km/s. It appears relatively unaffected by the presence of the kimberlite field. Extremely large P-wave velocity (>8.7 km/s) of the sub-Moho mantle is interpreted along profile I, except for a 70-km wide zone with a "normal" Pn velocity of 8.1 km/s below the kimberlite. Profile II mainly shows Pn velocities of 8.0–8.2 km/s, with unusually large velocity (>8.5 km/s) in two, ca. 100-km wide zones, at its southwestern end, one zone being close to the kimberlite field. The nature of these exceptionally large, sub-Moho mantle velocities is not yet understood. The difference in velocity in the two profile directions indicates anisotropy, but the effect of unusual rock composition, e.g. from a high concentration of garnet, cannot be excluded.

Keywords: Kimberlite; Siberian platform; Seismic velocity; Crust; Mantle

1. Introduction

There is uncertainty about how kimberlite pipes are being emplaced by eruptions of magma from deep in the upper mantle and very little is known about the deep

* Corresponding author. Tel.: +45 3532 2452; fax: +45 3314 8322.
E-mail address: thybo@geol.ku.dk (H. Thybo).

0040-1951/$ - see front matter © 2006 Elsevier B.V. All rights reserved.
doi:10.1016/j.tecto.2006.01.009

geologic structures of kimberlite fields. It is generally believed that kimberlite pipes penetrate the lithosphere from their source to the surface of the Earth with extreme speed (e.g. Haggerty, 1986; Boyd and Gurney, 1986). The bulk of kimberlite pipes are very small, which reduces our possibilities for detection and mapping of the magma path through the lithosphere by geophysical methods. Further, the physical parameters of solid kimberlitic rocks that have cooled near the surface of the Earth are often similar to the properties of the host rocks. This presents another challenge to geophysical imaging of the primary structures of the kimberlite fields. Much research has been devoted to identification of crustal geologic structures that may facilitate the intrusion of kimberlite pipes, such as major deeply reaching shear zones in the crust and uppermost mantle or crustal collision zones from early terrane amalgamation.

There are two major problems for application of geophysical methods to studies of the deep structure of kimberlite provinces: (1) to determine measurable physical parameters that may discriminate between kimberlite provinces and the surrounding regions, and (2) to identify geophysical anomalies, which are typical for kimberlite fields. Solving these problems involves studies of the original formation of the crust and lithosphere of Precambrian cratons and the subsequent, secular evolution of such regions, as well as rapid physical and chemical processes in the crust–mantle system. An important issue is how to trace geophysical anomalies laterally and correlate the measured anomalies to petrologic and geochemical data (e.g. Sobolev and Sobolev, 1971; Sobolev, 1974; Haggerty, 1986; Griffin et al., 1999; Pokhilenko et al., 1999).

The measured geophysical parameters of the crust and mantle in the kimberlite fields are often similar to the parameters of the surrounding, undisturbed cratonic regions. The differences in density, magnetic and electrical properties between kimberlites and other rocks are usually very small, such that potential field and electromagnetic methods mainly are useful for identification of features of the lithosphere, which are only indirect causes of the presence of the kimberlite pipes. The heat flow in kimberlite provinces is often small which indicates the existence of deep lithospheric keels. The identification of the extremely small geophysical anomalies related to kimberlite fields can only be accomplished by close integration of geophysical, petrological and geochemical data.

A series of seismic experiments for studies of the Yakutian kimberlite province by DSS methods with analogue seismic stations was carried out in the period of 1980–1995. The data indicate differences in the seismic structure of the crust and uppermost mantle between the kimberlite fields and the surrounding areas. Some crustal difference is inferred but has, so far, not been uniquely determined. Probably, unusually large seismic Pn velocities are the most distinct seismic observation around kimberlite fields. Velocities of up to 8.7 km/s have been reported for Siberia (e.g. Uarov, 1981; Suvorov et al., 1983) and 8.6 km/s for the Trans-Hudson Orogenic province in Canada (Nemeth and Hajnal, 1998).

Here, we present the results of interpretation of vintage DSS data from Siberia along two crossing profiles around the Mirnyi kimberlite pipe in Yakutia. We have digitized the data from the analogue recordings, which has allowed processing and plotting with modern methods, including the construction of record sections for the first time for this area. The processed data has been modelled by use of ray tracing techniques. The resulting models of seismic velocity along the profiles confirm the existence of the extremely large velocities, but the detailed modelling identifies also abrupt transitions to "normal" velocity of around 8.2 km/s. These results indicate that the extremely large velocities are caused by anisotropy from alignment of the olivine component of the mantle rocks. However, our detailed velocity models cannot uniquely confirm that anisotropy causes the large velocities of the sub-Moho mantle and it is possible that unusual mantle mineralogy in the region may cause the abnormally large seismic velocity. The models show reduction of the seismic velocity of the upper crustal rocks in the immediate vicinity of the kimberlite pipes inside a zone of elevated velocity over a lateral distance of 120 km. Our newly digitized seismic data has permitted the first detailed seismic interpretation of the crust and uppermost mantle around the Mirnyi kimberlite field.

2. Geological setting

The kimberlite province in Yakutia is located in the eastern part of the Siberian platform. Only five of the kimberlite fields, in the southern part of the province, include pipes that contain diamonds. These diamond-bearing fields are all of middle Palaeozoic age and are located inside the Siberian platform. The existing geological, geochemical and geophysical data suggest that the Siberian platform consists of a series of Archaean and Proterozoic crustal terranes, which were amalgamated during the Proterozoic and later underwent lithospheric extension during several stretching events (Rosen et al., 1994). Basement outcrops are found in the

Anabar shield and in the uplifted Hapschan–Birekte terranes. A series of Archaean and Proterozoic terranes (Fig. 1), which are separated by shear zones, in the eastern Siberian platform were defined from interpretation of magnetic and gravity anomalies, integrated with geologic data from crustal shear zones, boreholes to basement and crustal xenoliths. Some of the kimberlite fields are located at terrane boundaries, such as along the Billyakh Shear Zone, and other fields possibly may be located in the interior parts of the terranes.

Rosen et al. (1994) suggest that ~90% of the basement of the craton was extracted from the mantle during the Archaean before 3.0 Ga, followed by a 2.5–2.7-Ga orogenic event in the Magan and Anabar provinces. Ages of the Kotuykan and Billyakh Shear Zones suggest that the amalgamation of the northern part of the Siberian Craton took place between 2.0 and 1.9 Ga (Griffin et al., 1999). The stable area of the Siberian platform is surrounded by major Phanerozoic suture zones, which can be ascribed to the assembly of the Pangaea supercontinent.

The northern part of the kimberlite province includes the Hapschan, Birekte and Aekit terranes, separated by a thrust belt and a shear zone. The *Anabar province* consists of the Daldyn and the Markha terranes, which have been thrust southwestward over the Magan province. The Daldyn terrane is exposed in the Anabar shield, whereas the Markha terrane is not exposed at the surface. Three kimberlite fields have been identified close to the interpreted transition between the terranes.

The Mirnyi kimberlite is located within the *Magan province*. This province is bounded to the northeast by the Kotuykan Shear Zone, which is exposed as a 10–30-km wide deformation zone in the Anabar shield, and to the southwest by the Sayano-Taymyr Fault Zone, only recognized on the basis of potential field anomalies. The exposed basement rocks of the Magan province in the Anabar shield are high-grade granulites, mainly with felsic-intermediate igneous protoliths. All xenoliths from kimberlite pipes in the Magan province consist of similar rock types. Zircon data indicates crustal formation ages of ca. 3.0 Ga (Rosen et al.,

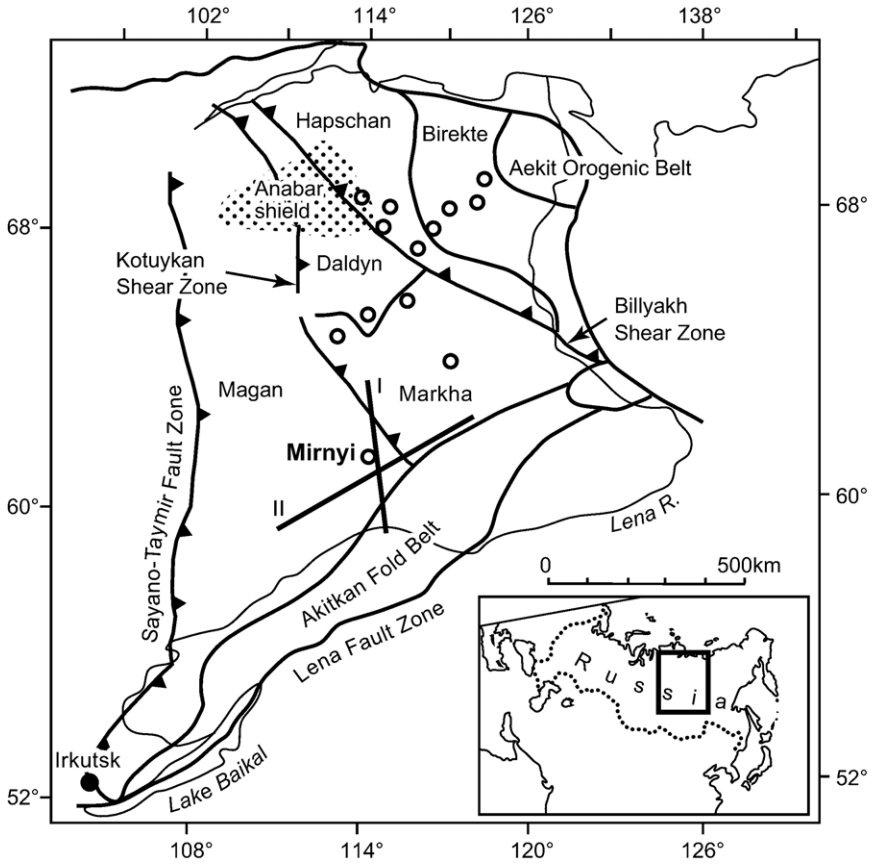

Fig. 1. Tectonic sketch map of the eastern part of the Siberian craton, which includes the kimberlite province with its diamond bearing kimberlite fields of Palaeozoic age (after Rosen et al., 1994). Kimberlite fields are shown by circles. Main terranes are named between shear zones. Thick lines show the locations of the DSS profiles I and II around the Mirnyi kimberlite field. Insert shows the location of the main map.

1994). The southward termination of the Magan and Anabar provinces follows the Lena Fault Zone, which marks the transition into the Proterozoic Akitkan Fold Belt.

The platform cover generally attains thicknesses of 2 km at the margins of the shields to 12–14 km in the Vilyui basin, which extends westward to close to the Mirnyi pipe. The platform cover consists of sedimentary rocks, which were deposited during the period from Riphean (Neoproterozoic) to Lower Cretaceous, as well as Triassic volcanic rocks. This > 1.2-Ga period included sedimentation in large aulacogens or rifts, which may be connected with epochs of extension, as well as in wide, regional basins, which may have formed in response to the loading of rift structures or to regional subsidence (Zonenshain et al., 1990).

There are no known kimberlite pipes that may be related to Riphean extension, although the occurrence of pyrope garnets in Palaeozoic beach placers in the SW part of the craton suggests that Precambrian kimberlites may exist (Griffin et al., 1999). All the Upper Devonian kimberlite pipes occur between the Devonian, EW striking Vilyui and Kyutungda aulacogens. The Mirnyi kimberlite pipe is located at the end of one of the branches of the Vilyui aulacogen, which contains up to 8 km of Upper Devonian and Lower Carboniferous rocks (evaporites and bimodal volcanics) below younger deposits.

Geologic studies of the Yakutian kimberlite fields has resulted in a comprehensive data base on the composition, mineralogy and structure of the crust and upper mantle around the kimberlite fields. The database includes samples of xenoliths from the kimberlite pipes and samples of basement rocks from wells (Sobolev and Sobolev, 1971; Sobolev, 1974; Safronov et al., 1990, 2001). Geophysical studies include interpretation of gravity and magnetic data (Erinchek et al., 1994; Manakov et al., 2000), remote sensing by use of satellite data (Brachvogel, 1984) and interpretation of magnetotelluric sounding (DSS) data (Manakov et al., 2000). Further, Deep Seismic Sounding data and CDP profiles have been acquired, processed and interpreted (Duhovskyi et al., 1986; Vaganov et al., 1995; Grinson, 1997; Karaev et al., 2000).

3. Previous geophysical investigations

Magnetic data has been vital for determination of the individual major terranes of the Siberian platform and as indication of the presence of main shear zones, which possibly locate kimberlite fields. There is rarely any distinct signature of kimberlite fields and pipes in the potential field data.

The Siberian kimberlite province is characterized by very low heat flow down to 25–30 mW/m^2, which indicates that the lithosphere may be up to 250–400 km thick (Duchkov and Sokolova, 1997; Artemieva and Mooney, 2001). This is in agreement with results from global seismic tomography, which indicates a lithospheric thickness of the order of 350 km (e.g. Zhang and Tanimoto, 1993), although regional surface wave tomography indicates a less than 200-km-thick lithosphere (Priestley and Debayle, 2003) in accordance with studies of xenoliths and kimberlitic rocks (e.g. Boyd and Gurney, 1986; Groves et al., 1987; Pokhilenko et al., 1999). Analysis of the gravity field gives indirect indication of a lithospheric keel under the southern part of the kimberlite province, where the diamond bearing kimberlites are located (Manakov et al., 2000).

A main hypothesis for geophysical determination of their location has been that kimberlite fields and pipes are mainly located at the sites of deep fault intersections, but application of this hypothesis has been hampered by strong signals from other sources, e.g. at shallow depth. The small contrast in density between kimberlites and the host rocks, e.g. Cambrian limestone rocks, precludes the use of gravity in Siberia. The magnetic field includes local anomalies from mafic dykes and magnetic patterns of the basement, which are strong compared to the effects from the, often, gentle magnetization of the kimberlites (Erinchek et al., 1994). Small resistivity values have been observed at kimberlite fields (Manakov et al., 2000).

Seismic studies of the kimberlite fields in Russia have mainly been carried out by use of Deep Seismic Sounding (DSS) methods, which determine the variation in velocity and depths to reflecting interfaces in the crust and uppermost mantle along profiles (e.g. Suvorov et al., 1997). Such studies often demonstrate strong variation in depth to intracrustal interfaces, in places the variations are five to seven times larger than those of the basement and Moho depths. Such strong variation may correspond to crustal collision zones from the original amalgamation of the craton. The relation in topography to major sedimentary strata has shown that intracrustal structures formed or were activate in middle Palaeozoic time (Suvorov et al., 1997). However, there is no conclusive evidence for relation to the emplacement of the kimberlite fields. Normal incidence seismic reflection data acquired with the CDP method indicates that crustal reflections are shallower at kimberlite fields than in the surrounding areas (Manakov et al., 2000). There is a tendency for identification of pronounced crustal reflectivity and scattered waves around the kimberlite fields (Karaev et al., 2000).

Probably, the most distinct seismic observation at kimberlite fields is the presence of unusually large seismic velocity of the Pn waves, which propagate directly beneath the Moho. Pn velocities as large as 8.5–8.7 km/s have been reported from several seismic studies of the kimberlite province in Siberia (Uarov, 1981; Suvorov et al., 1983, 1999) and at the kimberlite provinces of the Trans-Hudson Orogen in Canada (Nemeth and Hajnal, 1998). The most likely explanation for such large velocity is in terms of anisotropy of the sub-Moho rocks, but multidirectional studies indicate isotropically large velocities (Suvorov et al., 1999). However, lateral heterogeneity in the measured Pn velocity may complicate the interpretation of anisotropy.

4. Seismic data

4.1. Seismic experiment

We present the results from reinterpretation of explosion seismic data along two crossing Deep Seismic Sounding (DSS) profiles located in the southwestern part of the Yakutian kimberlite province (Figs. 1 and 2). The NNW–SSE striking profile I crosses the Mirnyi kimberlite field. Data acquisition took place in 1981 with 41 mobile stations distributed along a linear profile with a length of 380 km. Seismic waves were recorded from 20 explosions inside the recording array and one explosion at a distance of about 50 km to the southeast of the profile line. The southwest–northeast striking profile II crosses profile I at a distance of 30 km to the south of the kimberlite field near the centre of the recording line. Data were acquired in 1983 with 45 stations equally distributed along the 340-km long recording array. These stations recorded seismic energy from 17 in-line explosions and four explosions off the ends of the profile, out to 170 km beyond the recording line (Fig. 2). The shot point spacing along both lines was on average 20–22 km, varying between 10 and 30 km. The shot points outside the recording array allow accurate determination of the velocity of the refracted Pn wave from the sub-Moho part of the uppermost mantle. The intervals between shots and stations are of the same order of distance such that the data set is very well suited for interpretation of the velocity structure of the crystalline crust and uppermost (sub-Moho) mantle. The nominal spatial sampling distance of ca. 8–9 km along the studied profiles provides a subsurface horizontal resolution of the same order of distance,

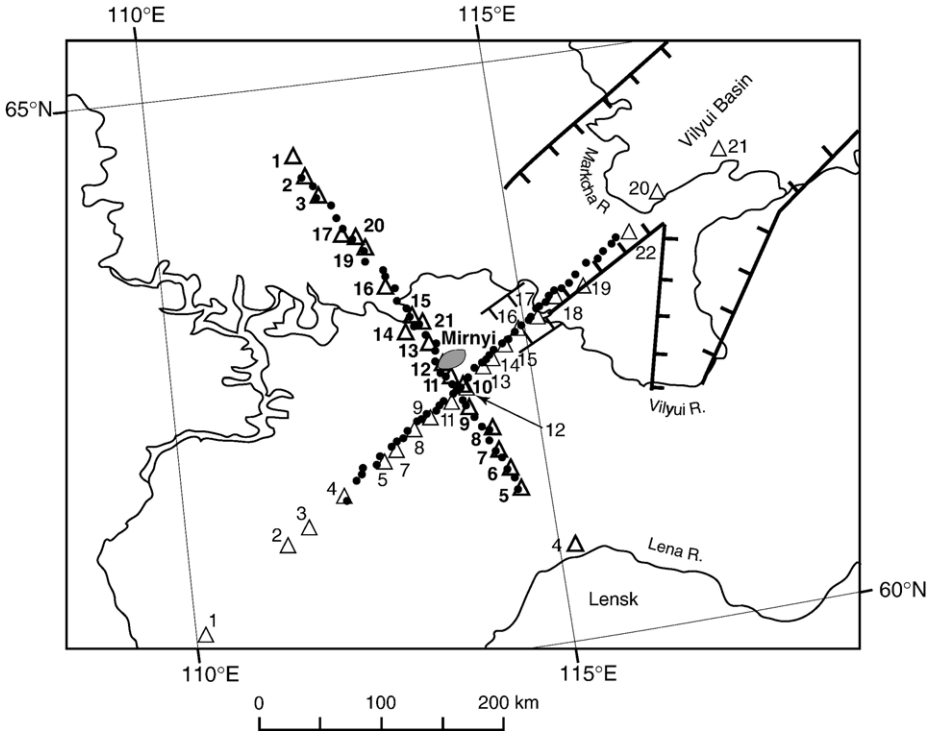

Fig. 2. Locations of the DSS profiles I and II around the Mirnyi kimberlite field. Triangles show shot point locations (bold for profile I); circles show locations of the recording station. The Mirnyi kimberlite field is shown by a grey ellipse.

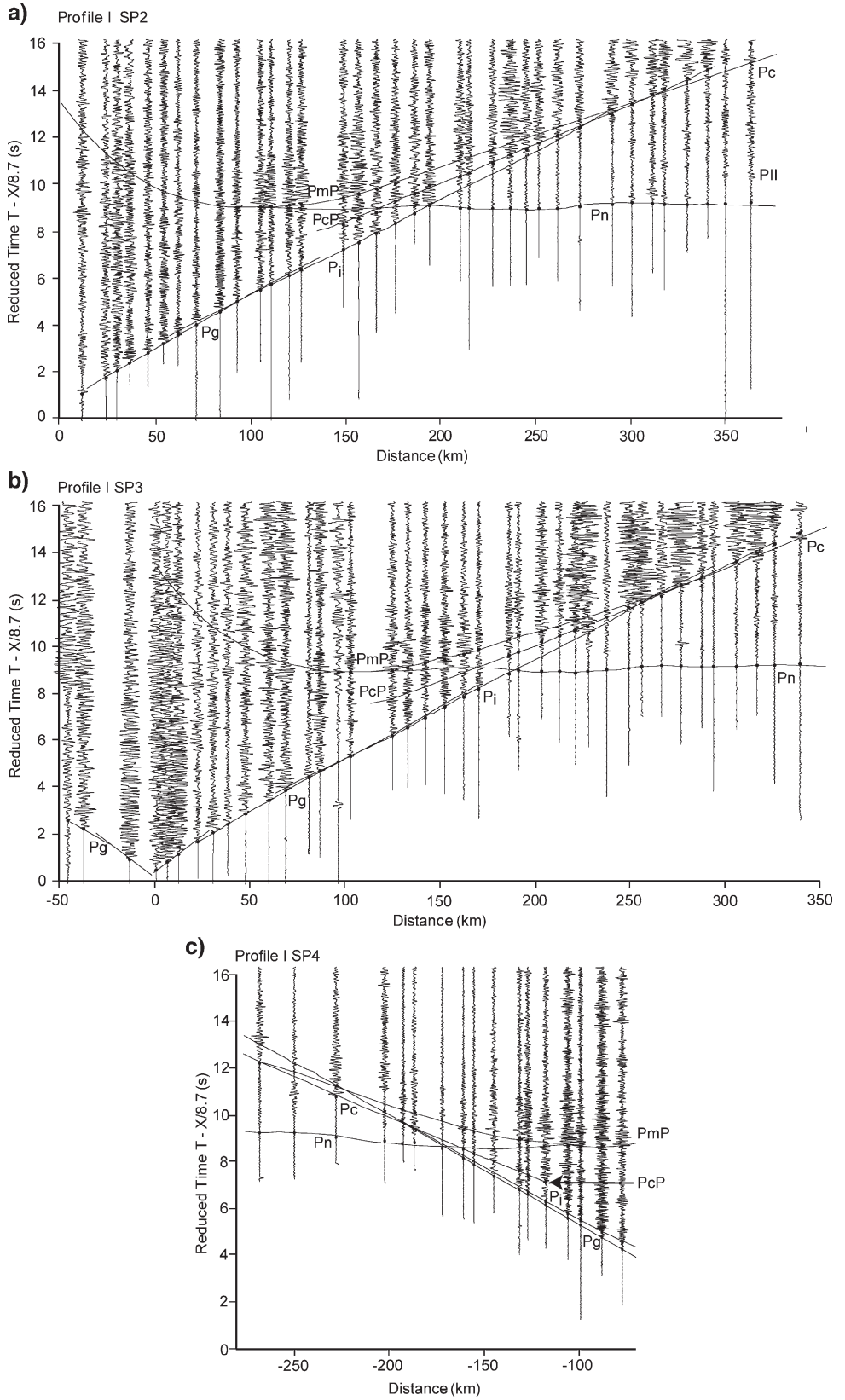
a)
Profile I SP2
Reduced Time T - X/8.7 (s)
Distance (km)
Pc
PII
PmP
PcP
Pn
Pi
Pg
b)
Profile I SP3
Reduced Time T - X/8.7 (s)
Distance (km)
Pc
PmP
PcP
Pn
Pi
Pg
Pg
c)
Profile I SP4
Reduced Time T - X/8.7 (s)
Distance (km)
Pc
Pn
PmP
PcP
Pi
Pg

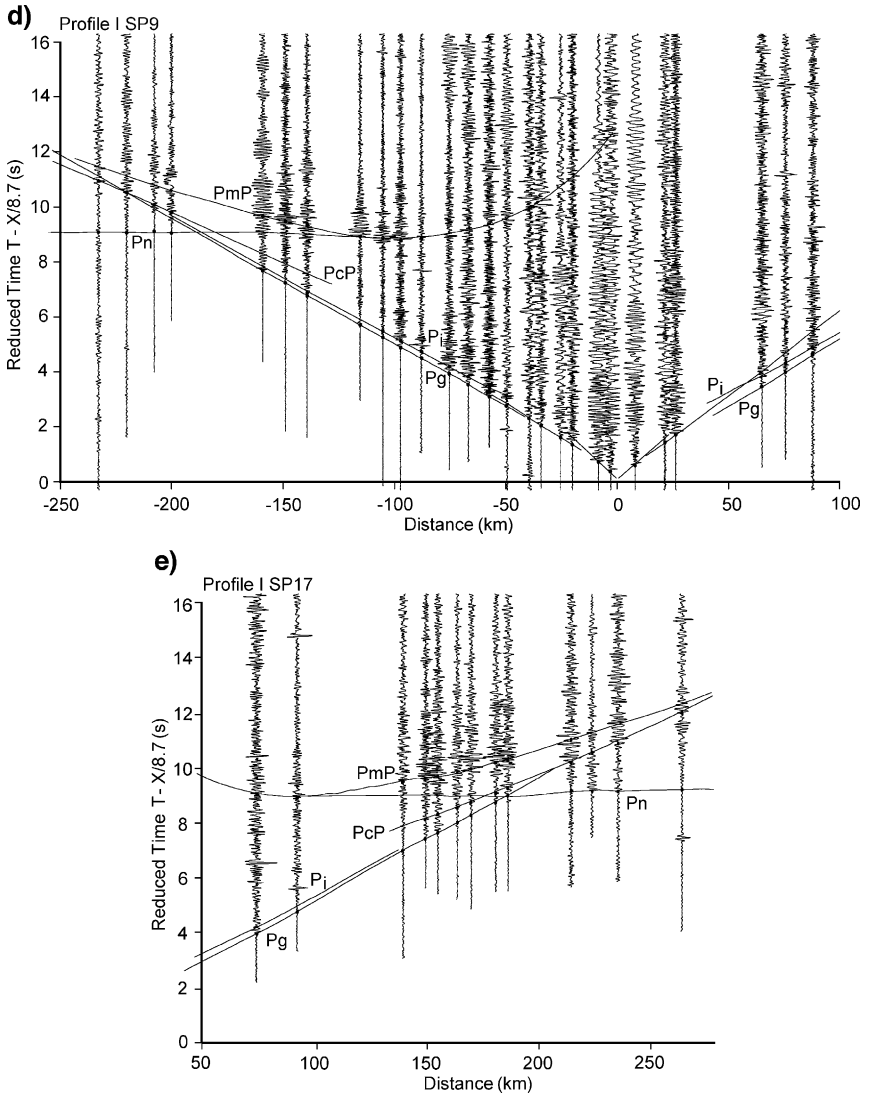

Fig. 3. Examples of amplitude-normalized seismic sections for selected shot points along profile I. Pg, Pi and Pn: refracted arrivals from basement, middle crust and the Moho, often observed as first arrivals. PcP and PmP: reflections from the major intra-crustal interface between the middle and the lower crust, and from the Moho. PI, PII are reflections from the upper mantle, which have not been modelled in this paper. Points illustrate the arrival times of main seismic phases. Lines illustrate the calculated travel time curves for the final model (Fig. 7). Notice the relatively small lower crustal velocity throughout the area. (a) Shot SP2, (b) shot SP3, (c) shot SP4, (d) shot SP9 and (e) shot SP17.

taking into account the relatively dense distribution of shot points and the high signal to noise ratio (Fig. 3).

The explosions were detonated in shallow water bodies at depths of 1.0–2.0 m. A series of dispersed groups of charges with individual weights of up to 100–200 kg TNT were distributed at regular intervals of 10–15 m. The total charge used for small explosions was 1500 kg for recordings out to offsets of 100 km, up to 3000 kg for recording in the offset interval of 100–200 km and 6000 kg for recordings at offsets beyond 200 km. These large charge sizes were used in order to ensure observation of accurate Pn velocities, which requires reliable identification of the first arrivals. The low density of seismic stations made it desirable to use large charges for this purpose.

The mobile seismographs were six-channel «Taiga» instruments with analogue magnetic recording and radio-controlled switches for triggering of the recordings. A seventh channel recorded encoded time. Six geophone groups were spaced at 100 m at each deployment site. This potentially allows determination

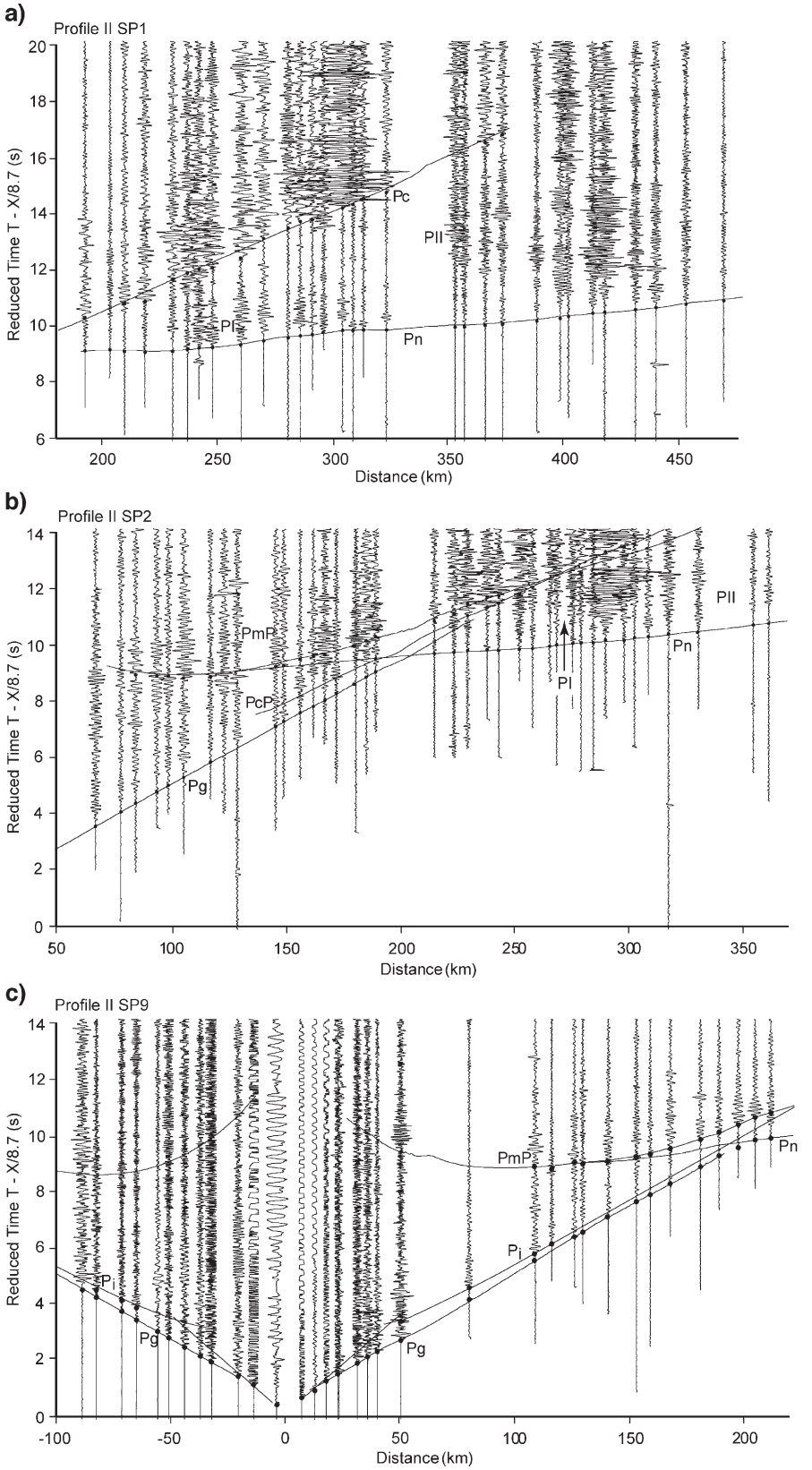
a)
Profile II SP1
Reduced Time T - X/8.7 (s)
Distance (km)
Pc
PII
PI
Pn
b)
Profile II SP2
Reduced Time T - X/8.7 (s)
Distance (km)
PmP
PcP
Pg
PI
PII
Pn
c)
Profile II SP9
Reduced Time T - X/8.7 (s)
Distance (km)
Pi
Pg
PmP
Pi
Pg
Pn

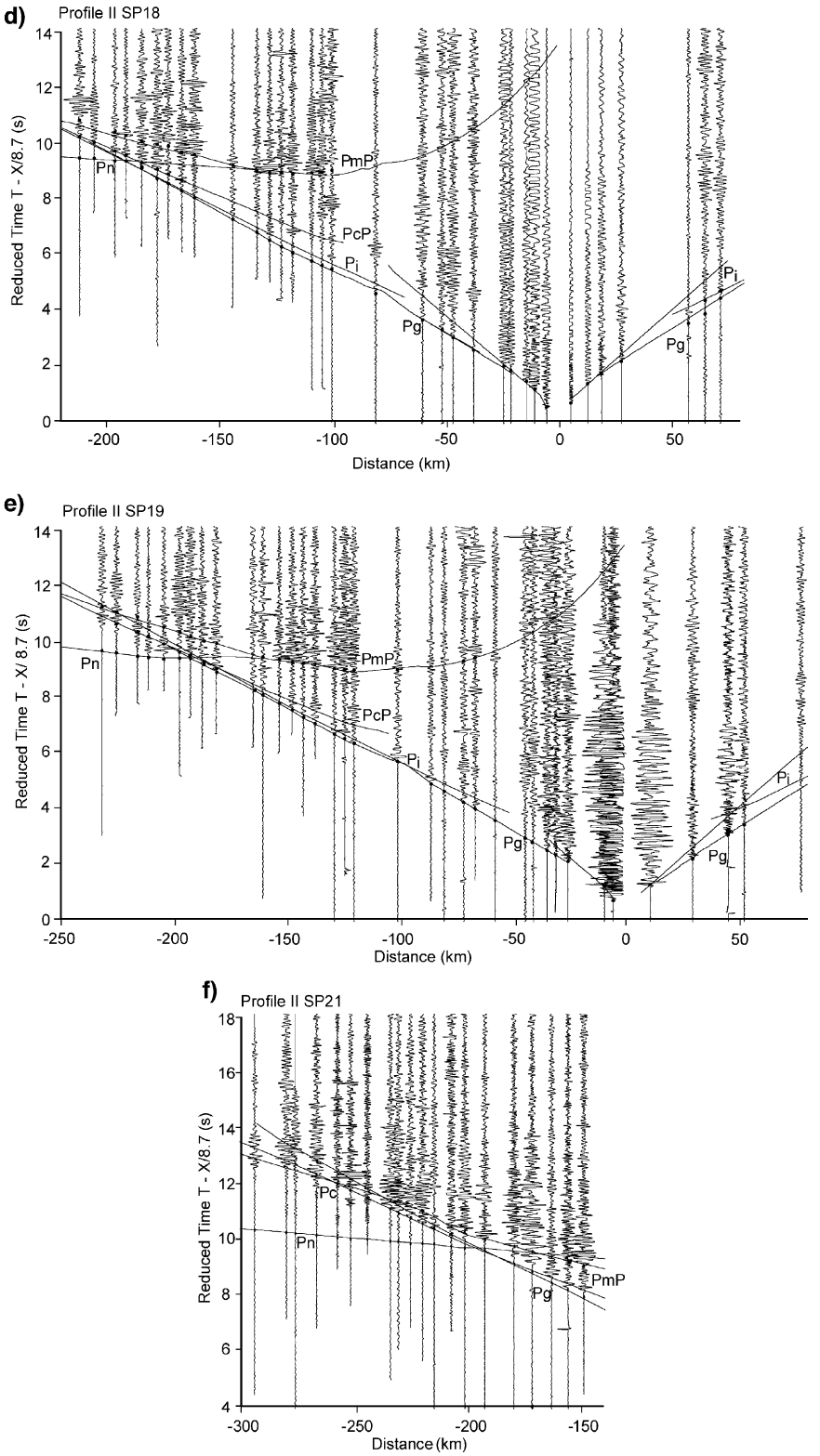

Fig. 4. Examples of amplitude-normalized seismic sections for selected shot points along profile II. Notation is explained in the caption for Fig. 3. Notice the relatively small lower crustal velocity throughout the area. (a) Shot SP1, (b) shot SP2, (c) shot SP9, (d) shot SP18, (e) shot SP19 and (f) shot SP21.

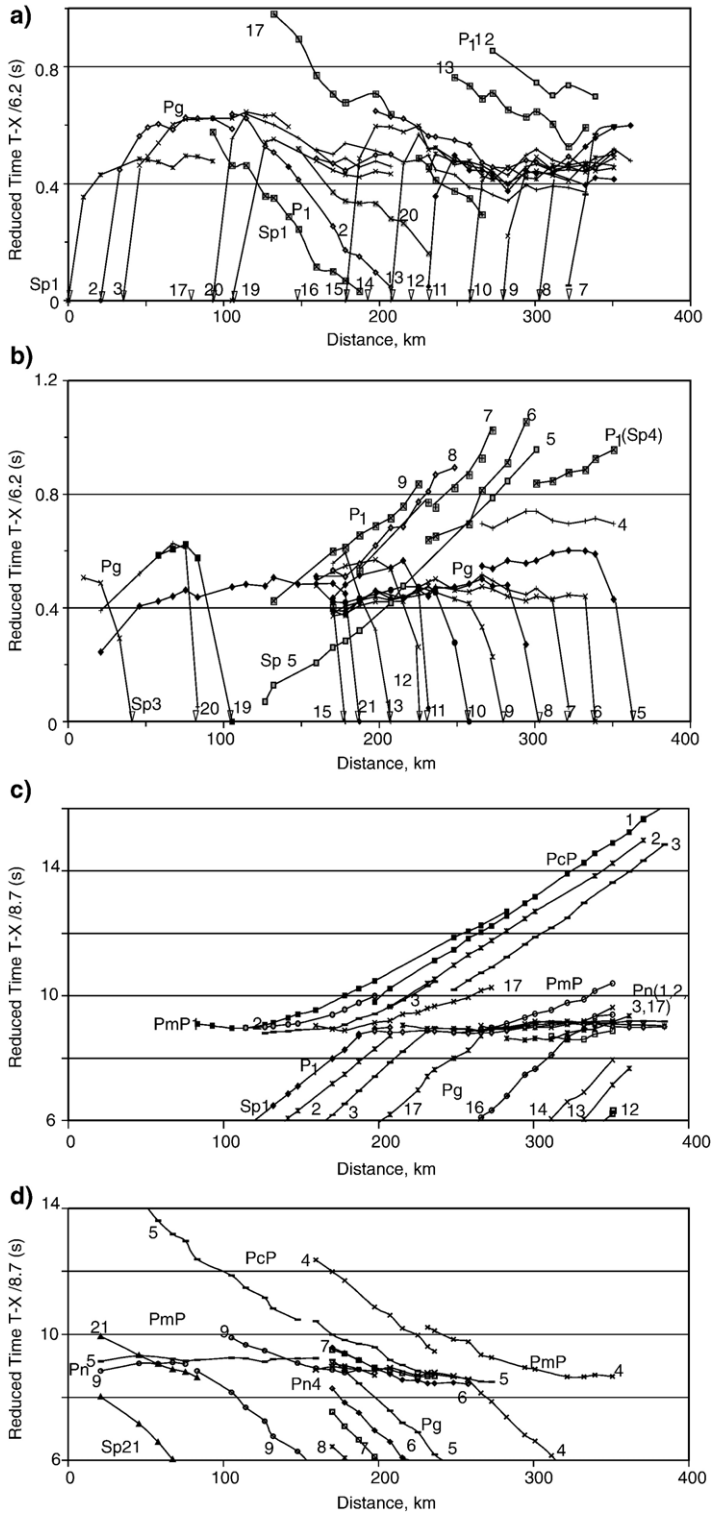

Fig. 5. Travel time curves along profile I of: Pg and P1 waves (southward in (a) and reversed in (b)), and Pn, PmP and PcP waves (southward in (c) and reversed in (d)).

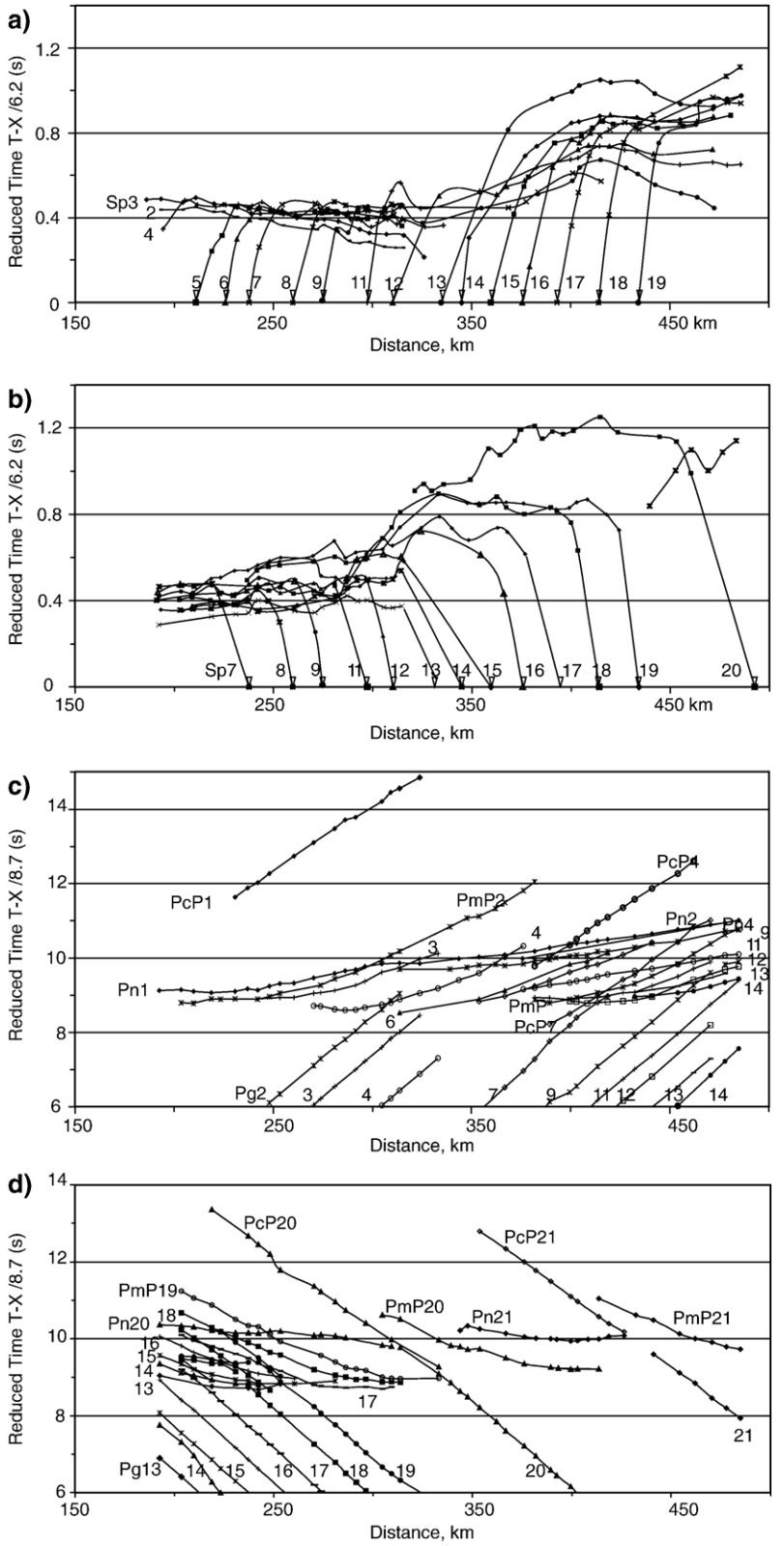

Fig. 6. Travel time curves along profile II of: Pg and P1 waves (southwestward in (a) and reversed in (b)), and Pn, PmP and PcP waves (southwestward in (c) and reversed in (d)).

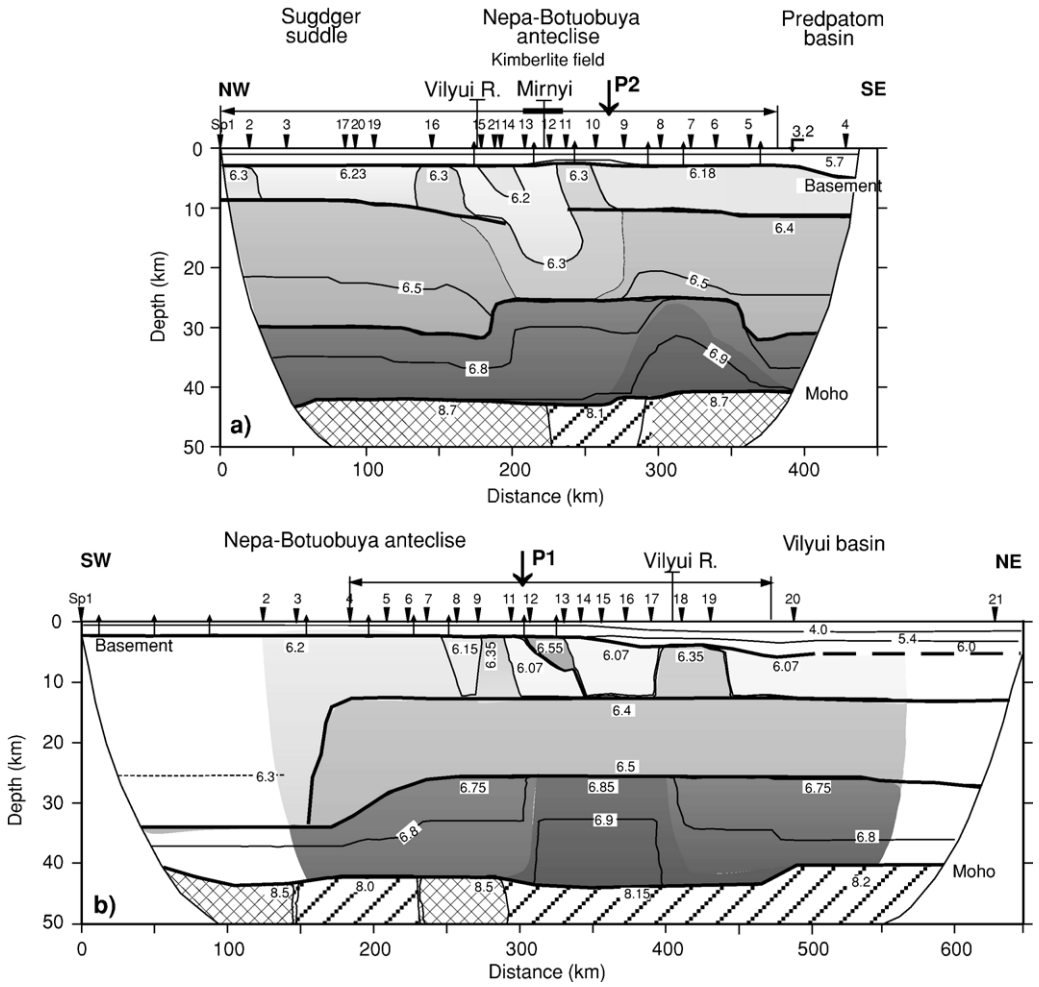

Fig. 7. Ray tracing derived velocity models of the crust and uppermost mantle along both profiles: (a) I and (b) II. Thick lines show seismic boundaries; thin lines are velocity isolines (km/s). The shaded region and gray scale are layers and intervals with differences in velocity. The locations of the Mirnyi kimberlite field and all shot points are illustrated. Notice the extremely large Pn velocity along most of profile I.

of phase velocities at each location as well as permits application of stacking procedures. Each channel recorded the signal from groups of eight serially connected geophones with a natural frequency of 5 Hz. The coordinates of the locations of recording stations and shot points were read from topographic maps in the scale 1:25 000.

We have recently carried out digitization with a sampling interval of 8 ms of about 95–98% of the original analogue recordings of the seismic signals. The data has subsequently been stacked within receiver groups and band pass filtered (3–28 Hz) wherever it was found desirable to increase the signal to noise level. Some of the original magnetic tape recordings were damaged. The resulting seismic data appear of very high quality and show several prominent seismic phases from the crust and uppermost mantle, including strong well-defined first arrivals to the farthest offsets.

4.2. Seismic phase correlation

The data is of very high quality and each record section shows energy propagation to the farthest offsets recorded along both profiles (Figs. 3, 4, 9 and 10) The crust is generally not very reflective. The seismic sections usually show two reflections from the crystalline crust and a strong PmP reflection from the Moho. This indicates a three-layered crust, typical for cratonic regions (Meissner, 1986; BABEL Working Group, 1993). The PmP waveform is mostly ringing with a coda, often longer than 2 s. An exception is in the central part of profile II in the distance interval of km 320–380 (Fig. 4), which is reversely covered by PmP reflections

from shot points 9 and 18. These PmP reflections are of relatively short duration. Some sections show rather strong reflections from the lower crust in a ringing band in front of the PmP reflection in the offset interval of 140 km to around 200 km, where the two reflections tend to merge. Therefore, this lower crustal reflectivity does not mask for identification of the PmP reflection, which generally has a critical offset of 100–110 km, indicative of a relatively constant crustal thickness along the two profiles.

The apparent velocity of the crustal refractions (Pg, Pi), interpreted from the gradient of the first arrival travel times, indicates large upper crustal velocity of the order of 6.2–6.3 km/s along most of both profiles, mainly along profile I. There is a remarkable variation in slope of the travel time curves along profile II. These first arrivals from the crust are identified out to 180–200 km offset where the Pn refraction from the uppermost mantle crosses over to become first arrival. The intracrustal refractions (or intracrustal, supercritical reflections, marked PcP) are observed to the end of the seismic sections as secondary phases, indicative of a maximum velocity of 7.0 km/s throughout the whole crust along both profiles.

The Pn refraction displays a different gradient along the two profiles. The apparent velocity is around 8.7 km/s along almost all of profile I. This apparent velocity is based on reversed observations, which show that the true velocity of the uppermost mantle must be around 8.7 km/s, at least to a few km below the Moho. The apparent velocity varies along profile II, where it is generally around 8.1–8.3 km/s with a few exceptions where it is 8.5–8.7 km/s. These observations are also reversed, such that they give precise indication for the true velocity of Pn propagation. These fundamental observations of strong difference in Pn velocity on two crossing, sub-perpendicular profiles, indicate that the uppermost mantle is highly anisotropic around the Mirnyi kimberlite field, although the evidence is non-conclusive.

Some sections show strong phases, which may be interpreted as reflections from the uppermost mantle (PI and PII). These reflections mainly appear at the ends of the profiles and have not been modelled in this study.

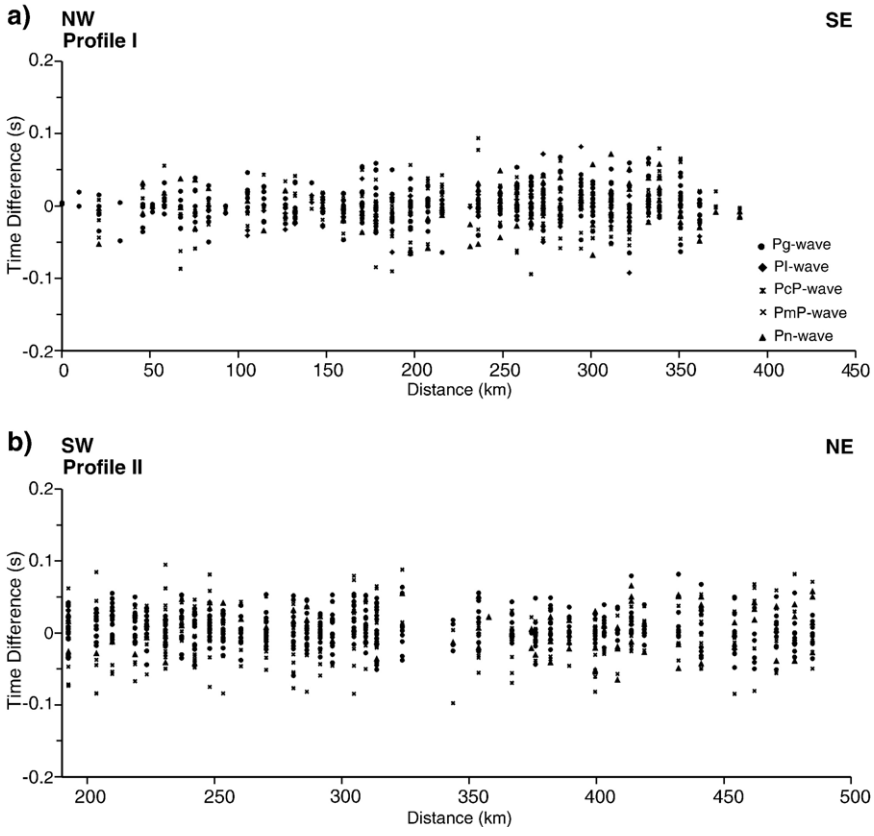

Fig. 8. Illustration of the obtained residual between picked and calculated travel times for the final models along profiles I and II.

5. Modelling procedure

The high quality of the seismic data has allowed identification of the onset of the seismic phases by group correlation of the refracted and reflected waves on almost all seismic sections. The travel times of the individual phases (shown by dots in Figs. 3 and 4, and plotted for all shot points for each profile in Figs. 5 and 6) have subsequently been picked by use of an interactive program. The compilation of travel times (Fig. 5) indicates a laterally fairly homogeneous crustal structure along profile I, where the sets of travel time curves clearly demonstrate the large velocity of the Pn phase along the whole of profile I (notice that a reduction velocity of 8.7 km/s is used in Fig. 5). However, the compilation of travel times for profile II indicates pronounced lateral variation of Pg and Pn velocity (Fig. 6), but not crustal thickness.

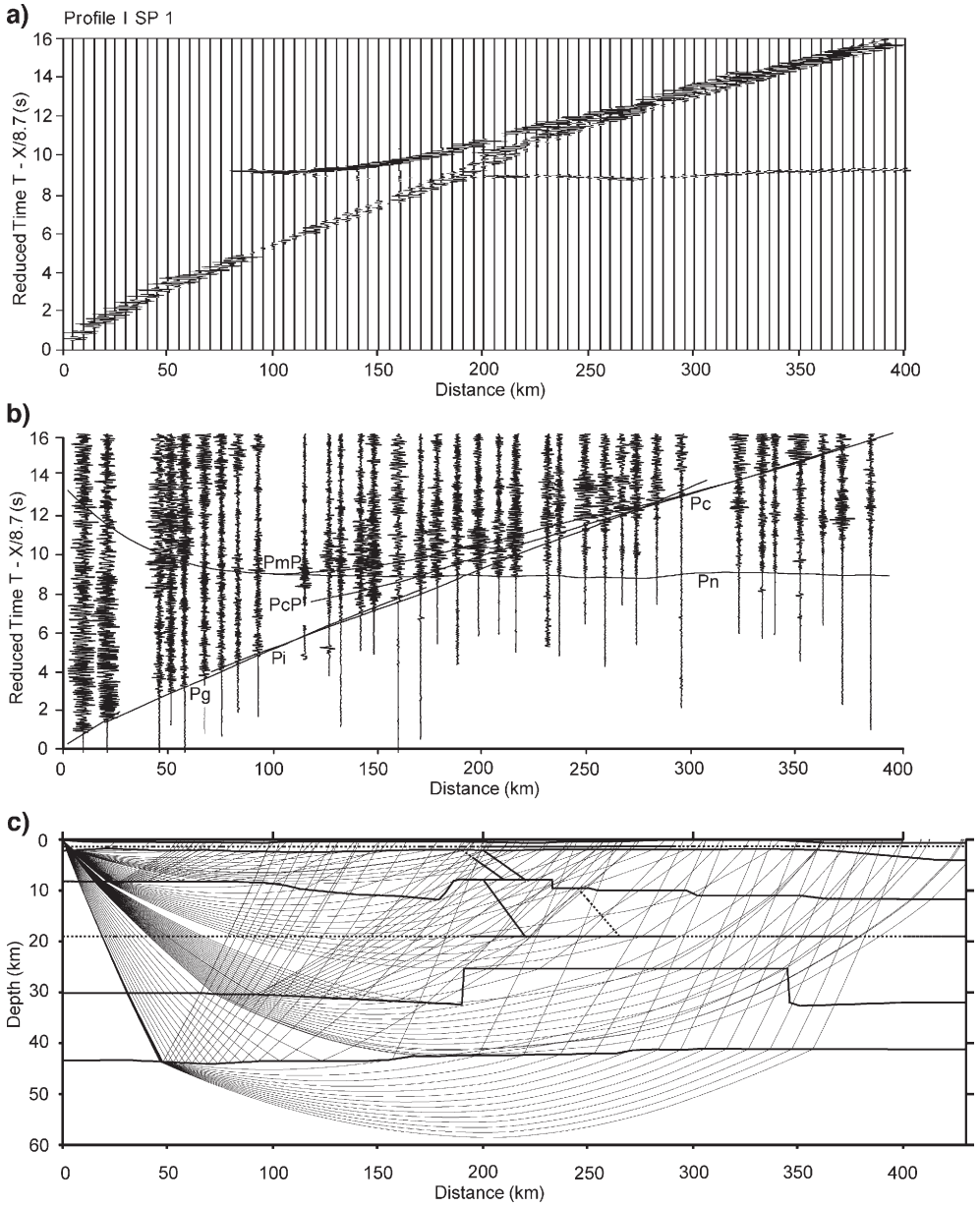

Fig. 9. Illustration of the ray tracing modelling results along profile I for shot points 1 and 5 as calculated for the final model in Fig. 7. (a and d) Synthetic seismic sections for the two shot points; (b and e) the observed seismic sections with picked travel times (points) and calculated travel times superimposed; (c and f) ray diagram for the two shot points. Reduction velocity is 8.7 km/s.

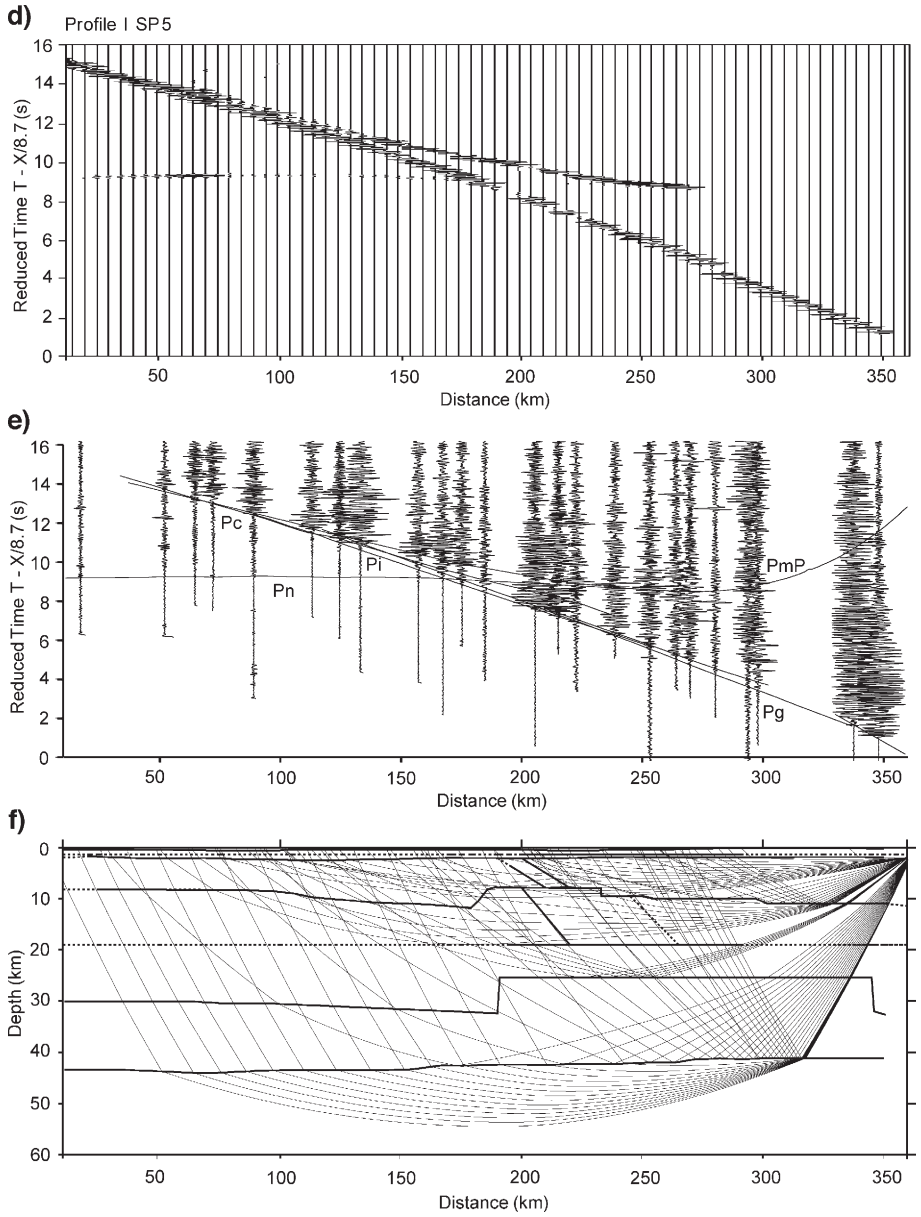

Fig. 9 (*continued*).

The two-dimensional models for profiles I and II (Fig. 7) were derived by forward travel time modelling by use of the ray tracing modelling program RAY84PC (Thybo and Luetgert, 1990). The models define the seismic velocity in a series of layers defined by surrounding boundaries with almost arbitrary depth variation defined by a series of node points, which extends across the whole model. The program calculates theoretical travel times for selected seismic phases, which can be compared to the readings from the seismic sections. The modelling procedure was based on the top-down approach, by first constraining the immediate subsurface part of the model and then step-wise iteratively determining the seismic velocity in deeper layers. At a late stage of the modelling procedure, the models were refined by comparison of calculated synthetic seismograms with the recorded seismic sections. The initial models were used to trace seismic rays from each shot point to each receiver along the profiles. The models were improved based on comparison of the theoretical and the observed travel times, and the seismic rays and travel times were recalculated. This

procedure was repeated many times, until an agreement between calculated and observed travel times was obtained within the assumed uncertainty of the data (0.05 to 0.1 s).

The first stage of the modelling procedure was definition of the basement topography which is a critical process for the quality of the subsequent modelling, in particular for the relatively coarse spatial sampling that is available in the current data set. The initial basement surface was constrained from well data together with seismic velocity models by Suvorov et al. (1983, 1986). It was subsequently modified at a few locations in order to produce theoretical travel times in agreement with the observed data. Comparison of calculated and observed travel times permits improvement of the models, for which seismic rays and travel times were again calculated. This procedure was repeated until calculated and observed travel times agree within 0.05–0.1 s. The residual travel times for all readings (Fig. 8) demonstrate the uncertainty of the models. An rms value of 60 ms for

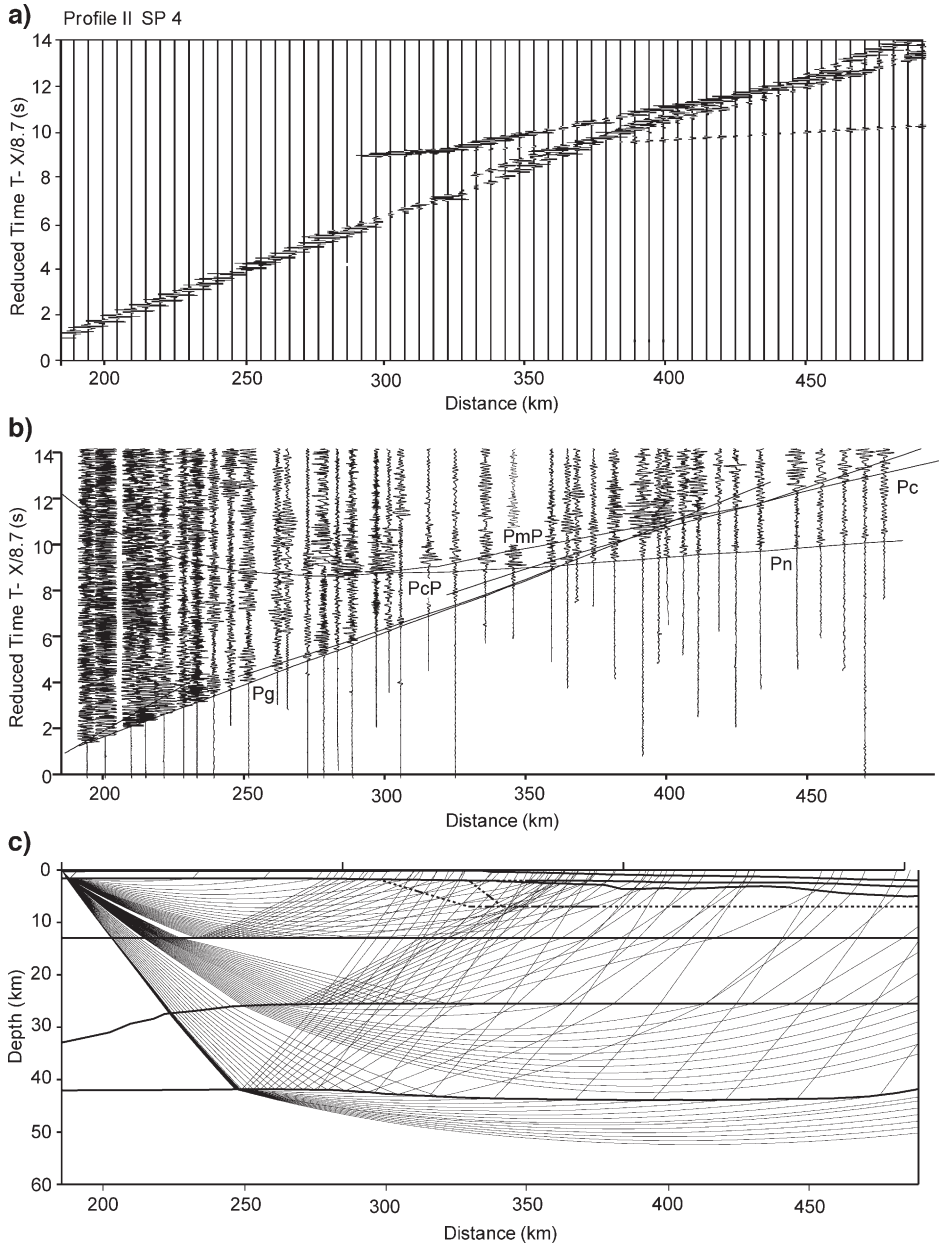

Fig. 10. Illustration of the ray tracing results along profile II (see caption to Fig. 9). (a, b, c) For shot point SP4 and (d, e, f) for reversed SP20.

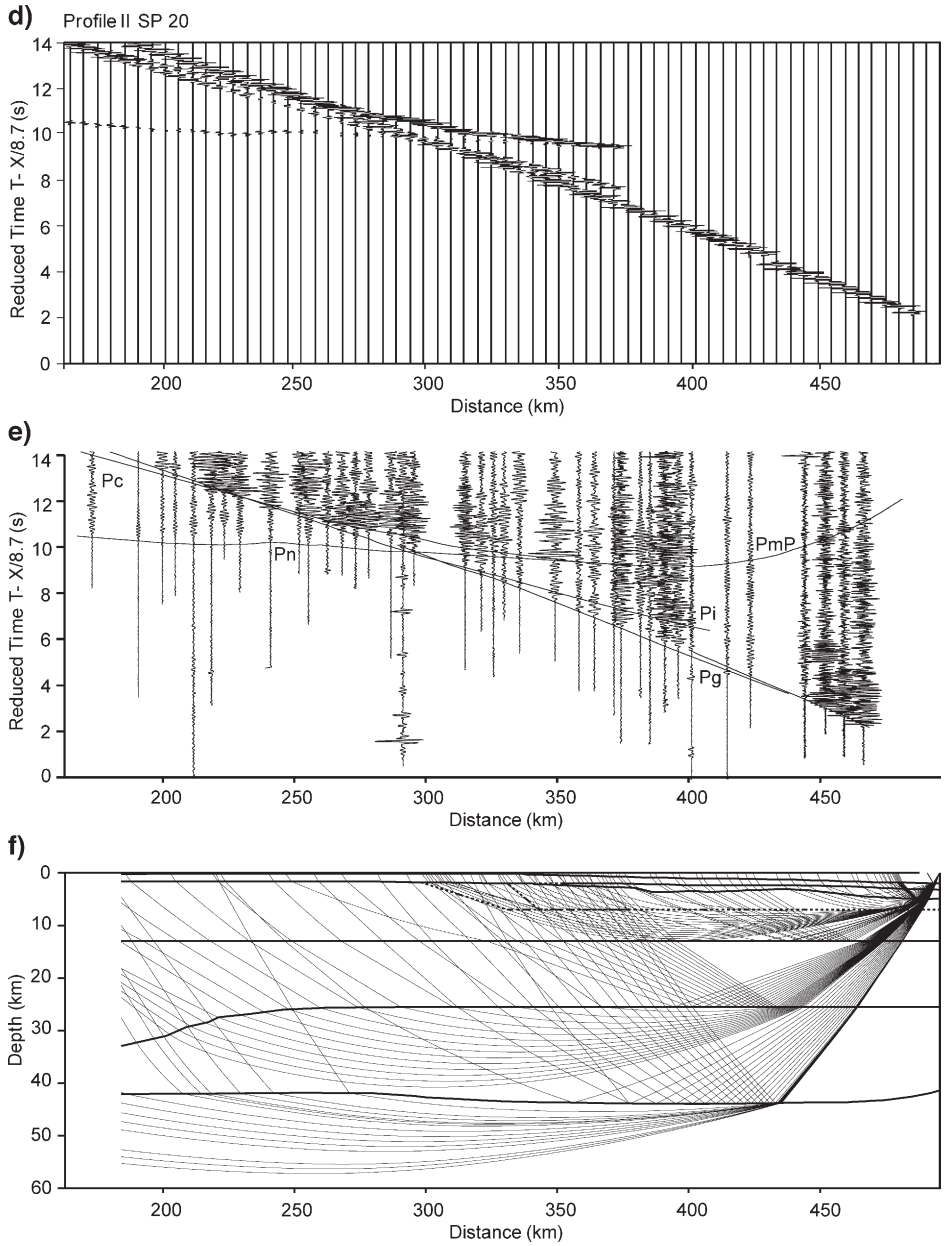

Fig. 10 (*continued*).

the residual travel times was achieved for the final model.

The model includes major intracrustal seismic boundaries along the whole profiles. Their depths are primarily determined from the corresponding reflections, although refractions from below the uppermost interfaces occasionally are first arrivals, in particular from below the first intracrustal layer. The final stage of the modelling included calculation of synthetic seismograms for the velocity models with RAY84PC. Comparison with the observed seismic sections allows adjustment of the velocity gradients within each layer and the velocity contrasts across the seismic interfaces. The synthetic seismic sections show fair agreement with the data sections (Figs. 9 and 10).

6. Documentation of the seismic models

The presence of the Mirnyi kimberlite appears to affect the seismic velocity structure of the upper and

middle crust down to a depth of 25 km along profile I. The seismic velocity of the upper and middle crust is larger (>6.3 km/s) than in the surrounding parts of the profile in ca. 20-km wide belts surrounding a 50-km wide zone at the kimberlite field with only slightly elevated velocity (>6.2 km/s). This zone extends through the middle crust to a depth of 25 km with a width of 50–80 km. There is no direct evidence of the presence of the kimberlite field in profile II, which has a distance of ca. 30 km to the pipe. However, the upper crust in this profile is very heterogeneous in a ca. 200-km wide zone around the kimberlite pipe, mainly extending toward the northeast, whereas the middle crust appears extremely homogeneous.

The overall crustal structure along the two profiles is similar, in particular regarding the rather uniform velocities of the middle and lower crust of 6.4–6.5 and 6.75–6.9 km/s, respectively. Zones of 50 km width with slightly (+0.1 km/s) elevated velocity have been modelled in the lower crust of both profiles. There is some variation in the depth to the lower crust in both profiles. The middle crustal layer, with velocities of 6.4–6.5 km/s, has been modelled with slight variation in thickness. The middle crustal layer thickens northwestward along profile I and it is absent at the southwestern end of profile II. These features are both well-documented aspects of the models.

The uppermost mantle part of the two models shows the strongest variation in seismic velocity. Underneath the fairly flat Moho in the area, the seismic Pn velocity ranges from 8.0 to 8.7 km/s along the two profiles. The largest velocity is mainly interpreted along profile I, where it extends along the whole profile except for a 70 km long stretch with a substantially lower velocity of 8.1 km/s. Abnormally large mantle velocity along profile II is only interpreted in two short stretches of 75–100 km length. Otherwise, the Pn velocities along profile II are in the range of 8.0–8.2 km/s.

Calculated travel times superimposed onto the data sections demonstrate that the velocity models explain the observed data for both profiles (Figs. 3 and 4). The root-mean-square (rms) misfit between the picked (observed) and theoretical travel times for the two models is around 60 ms for both the final models (Fig. 7). The misfit is very homogeneous along the two profiles (Fig. 8). We document the model quality by superimposing picked and calculated arrival times for the illustrated seismic sections (Figs. 3 and 4) as well as by illustrating the ray coverage and synthetic seismic sections for selected shot points (Figs. 9 and 10).

First arrivals from the sedimentary cover are observed only on a few traces close to the shot points. Slight adjustment to the initial model, which was based on borehole information made the refractions from the sedimentary strata and the Pg refraction from the basement fit to data sections. Substantial delay of the Pg phase at the northeastern end of profile II indicates the dip of the basement toward the Vilyui basin (Fig. 4a,b).

The Pg refracted wave from the basement is generally observed out to offsets of 100 km, where it is crossed by the Pi refracted wave from the middle intracrustal layer with a velocity of 6.4–6.5 km/s in profile I (Fig. 3). The velocity of the basement is on average slightly larger than 6.2 km/s. There is some scatter along profile I, which define lateral variation in the velocity between 6.2 and 6.3 km/s (Fig. 5a,b). Most seismic sections show a reflection just behind the Pg wave at offsets of 60–100 km, which merges with the first arrival Pi wave (Figs. 3 and 4). This demonstrates the existence of a wide-angle reflector at the top of the middle crust, which is observed along both profiles except for around the kimberlite field in profile I and in the farthest southwestern end of profile II. The basement velocity is variable along profile II with an average around 6.2 km/s. Inclusions with larger velocity (6.3 km/s) and even the extremely large velocity of 6.55 km/s over 30 km are well documented by the first arrival times (Fig. 6a,b). The Pi phase is not observed as first arrival along profile II and can only be correlated as secondary arrival (Fig. 6,d).

The velocity structure around the kimberlite field along profile I shows surprisingly small velocities in the centre part of the anomaly, surrounded by slightly elevated velocities of around 6.3 km/s in the upper crustal layer (Fig. 7). The low-velocity anomaly extends to the base of the middle crustal layer at depths of around. 25 km. This velocity variation is well constrained by the dense coverage of reversed observations of refracted first arrivals (cf. the undulations in arrival times around km 200 in Figs. 5 and 10).

Mainly the Pc refraction defines the velocity of the lower crustal layer. This phase merge with the PmP reflection at very far offset as the strongest observed phase. This provides strong evidence for a lower crustal velocity of 6.8–6.9 km/s and that no lower crustal layer of substantial thickness (thicker than ~3 km) may be present with velocity larger than 7.0 km/s. There is evidence for variation toward slightly elevated velocity in the lower crust around the kimberlite field. The PcP reflection from the top of the lower crust is relatively strong in many sections (Figs. 3 and 4) where it marks the onset of a reflective coda in front of the PmP reflection, indicative of a reflective lower crust (cf. Sandmeier and Wenzel,

1990; Thybo et al., 1998). Such strong reflectivity in wide-angle seismic data has recently been observed in other cratonic regions (e.g. Thybo et al., 2003). The reflective lower crust has made it possible to explain all the aspects of the, so-called, enigmatic teleseismic Pn phase, which has been observed in Russian PNE data (Nielsen and Thybo, 2003). The PcP reflection arrives 1–2 s later in the section for shot point 1 than for shot point 4 along profile II (Figs. 4 and 6c). This documents the abrupt downwarping of the lower crustal reflector at the southwestern end of profile II. The PmP reflection from the Moho is pronounced in all sections with high amplitudes in most sections in the offset interval of 90–180 km. This phase is often trailed by a long coda, indicative of heterogeneity below the Moho.

The significant variation in the velocity (8.0–8.7 km/s) of the uppermost mantle is well documented by clear refracted Pn phases, observed as first arrivals at offsets between 200 and 400 km (Figs. 3–6). These waves are observed over large parts of the models for reversed recordings, such that the velocity variation is known

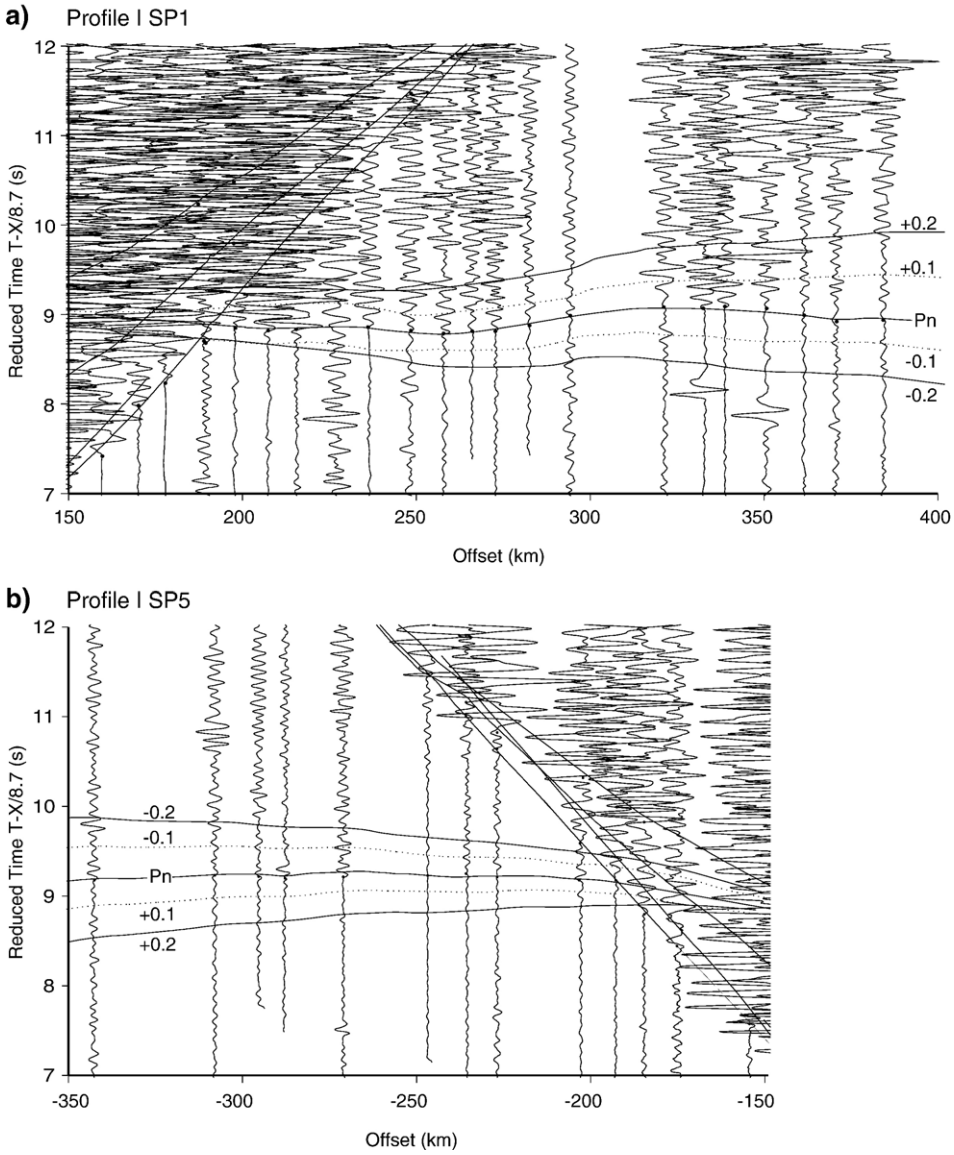

Fig. 11. Illustration of the uncertainties of the Pn velocities. Travel times are superimposed onto two sections along both profiles for the preferred model and for mantle velocities, which have been lowered as well as increased by 0.1 and 0.2 km/s compared to the seismic model (Fig. 7) with all other parameters kept constant. The figure demonstrates that the average Pn velocity has been resolved with an uncertainty smaller than 0.1 km/s.

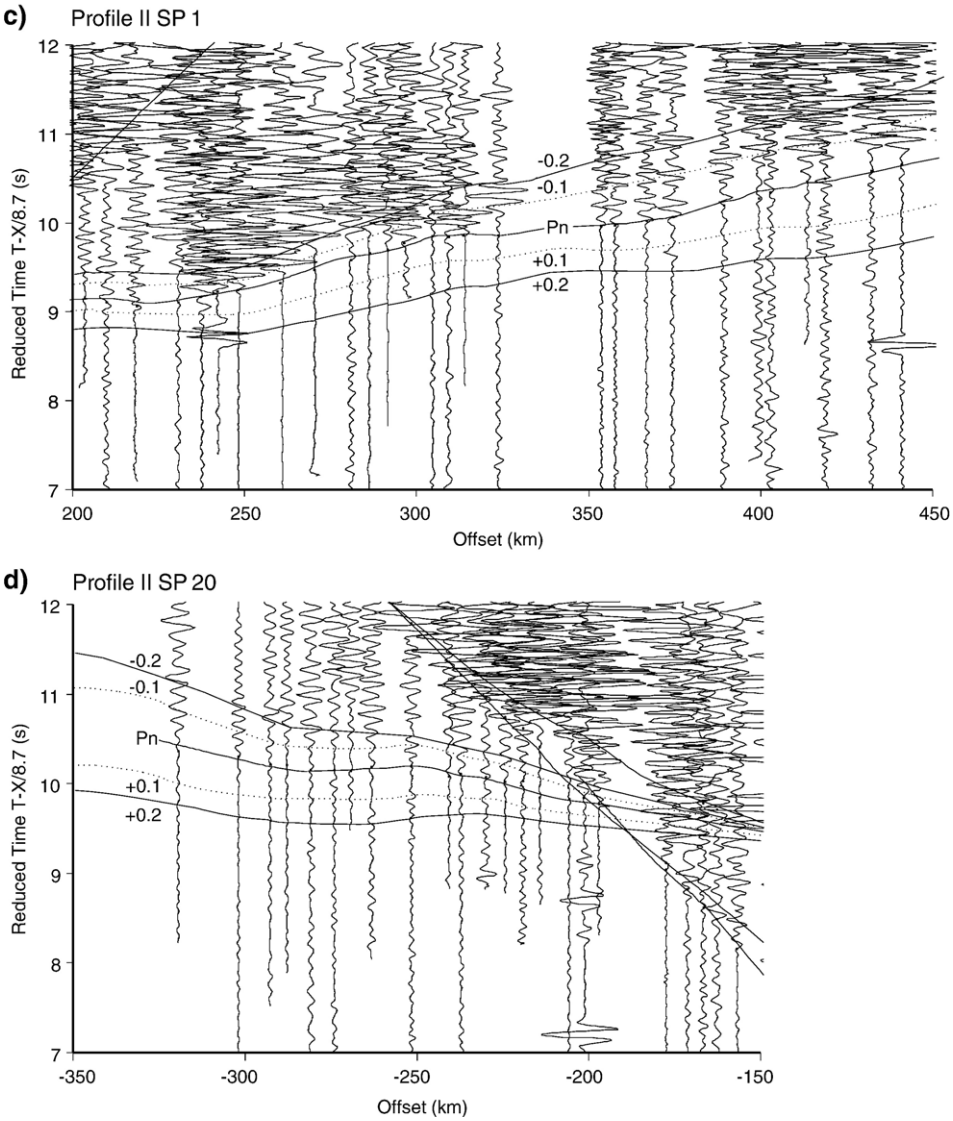

Fig. 11 (*continued*).

with a horizontal resolution, which is finer than 20 km. Most of profile I shows a Pn velocity of 8.7 km/s. This is very well documented by the observed Pn wave field. The modelling has shown that this velocity is known with an uncertainty, which is less than 0.1 km/s (Fig. 11). The large velocity is very well constrained as it extends along almost the whole profile. The Pn velocity is small (8.1 km/s) in a 80-km wide interval between km 225 and 285, which corresponds to the downward projection of the upper crustal low-velocity anomaly to the Moho. This feature is documented by a substantial delay in the Pn arrival (Fig. 3a), only observed in a southeasterly direction due to too short offsets from the shot points to the northwest. The reversed arrival times between the two directions and the delay of the Pn compared to the PmP phase in the section for shot point 5 (Fig. 3) adds credibility to this interpretation.

The Pn mantle velocity of 8.2 km/s along most of profile II is well documented by the general slope of the Pn phase (Figs. 4 and 6c,d). However, large Pn velocities of 8.5–8.7 km/s are also observed in two 55–80-km wide intervals along profile II (Figs. 4, and 6c,d), for example in the record section from shot point 1 over an 80-km wide interval at the southwestern end out to 235 km (Fig. 4a), and by the sections from shot points 19 and 20 over a 55-km wide interval between 290–340 km close to the intersection with profile I. As such, the strong lateral variation in both

profiles at the cross point is also documented. The abrupt lateral changes occur over intervals, which are narrower than 20 km; otherwise, the observed variation in travel time cannot be explained. The observations of the Pn phases are made in areas where the PmP arrival times are almost constant, which shows that the Moho is sub-horizontal. Therefore, the interpreted velocities of the uppermost mantle also are very reliable, cf. also Fig. 11.

7. Interpretation of the velocity models

The sedimentary cover has been modelled by two main layers. The upper layer has a mean velocity of about 3.2 km/s and a thickness 0.1–0.6 km. It is interpreted as mainly upper Cambrian limestone rocks, which possibly have been subject to weathering effects. The underlying limestone rocks of lower Cambrian age have a velocity about 5.6 km/s and a thickness of up to 1.5–2.0 km. The depth to the Archaean basement is 2–2.4 km in the platform proper. There is slight deepening of the basement to 4–5 km depth in the southeastern end of profile I at the Predpatom basin as well as in the northeastern part of profile II, where the basement of the Vilyui basin extends to depths of 5–6 km.

Both velocity models include three main layers in the crystalline crust with generally the same velocities: 6.0–6.35 km/s in the basement between 2–6 km and 10–13 km depth, 6.4–6.55 km/s in the middle crust to depths of 25–30 km and 6.75–6.9 km/s in the lower crust to depths of 40–42 km with a tendency toward slightly elevated velocity in a part close to the kimberlite field. The exceptions are lateral variation in the basement velocity around the kimberlite field, and the existence of a 30-km wide inclusion with a velocity of 6.55 km/s in the central, upper crustal part of profile II close to the Mirnyi kimberlite field. The velocity model indicates the absence of the middle crustal layer in the Nepa-Botuobuya anteclise in the southwestern part of profile II. The general three-layered crust appears to be typical for Precambrian shields (Meissner, 1986; BABEL Working Group, 1993), although the crustal thickness of ca. 42 km in the area around Mirnyi is smaller than in other platform areas (e.g. Thybo et al., 2003). The observed mantle reflections (PI, PII) appear to arrive at approximately the same offsets and times as in sections from other cratons (BABEL Working Group, 1993).

The basement velocity is generally around 6.2 km/s except for localised anomalies with velocities up to 6.55 km/s. The lateral variation in basement velocity along profile I coincides with the Mirnyi kimberlite field. The abrupt, significant lateral variation along profile II may partly be ascribed to the transition between the Magan and Anabar provinces, which is located around shot points 17 and 18 and coincides with the transition into the Vilyui basin. The basement velocity beneath the Vilyui basin (in the Anabar province) is less than 6.1 km/s. The localised high-velocity anomalies (6.35 and 6.55 km/s) around km 280, 320 and 410 may be related to magmatism at the kimberlite field. The middle crustal velocity structure appears very homogeneous compared to the heterogeneous upper crustal structure. The basement of the Nepa-Botuobya anteclise in the southwestern part of profile II is slightly elevated to a depth of 2 km above an anomalous crystalline crust, which only consists of two main layers with velocities corresponding to the upper and lower crust in other parts of the region.

The variation in crustal thickness along profile I is very gentle with a gradual deepening from 40 to 43 km toward the northwest. There is slight gradual variation in crustal thickness between 40 and 45 km depth along profile II with an abrupt uplift of the Moho from 45 km depth beneath the platform to 40 km underneath the Vilyui basin. There is some abrupt variation in the depth to the lower crustal layer between two constant levels at 25 and 30 km depth. Absence of reflections from the base of the upper crustal layer in a 40-km wide interval between km 200 and 240 occurs along profile I at the velocity anomalies surrounding the kimberlite field. This may be attributed to penetration by the kimberlite pipes through the crystalline crust in the area. However, no similar observation has been made for neither the top of the lower crustal layer nor the Moho.

The Pn velocities of 8.7 km/s in the uppermost mantle are unusually large as observed along most of profile I and along two parts of profile II. The abrupt changes in mantle velocity take place over narrow horizontal intervals of widths less than 20 km. The large velocities along profile II are not as well constrained as for profile I, but they must be larger than 8.5 km/s. The relatively small average Pn mantle velocity of 8.2 km/s along profile II indicates that the sub-Moho mantle consists of anisotropic material with at least 4% difference between the fast and the slow axes. As we only have velocity information along two almost perpendicular profiles, it is not possible to determine the absolute degree of anisotropy. The strong variation in Pn velocity along both profiles at their cross point makes it possible that we are observing extremely large bulk, isotropic

velocity in separate blocks or terranes, which is not necessarily caused by anisotropy.

8. Discussion

The crust around the Mirnyi kimberlite field is characterized by substantial lateral and vertical seismic heterogeneity, mainly expressed as abrupt changes in velocity in the upper crust and the uppermost mantle as well as changes in topography of first order seismic discontinuities. It is remarkable that the middle and lower crustal layers appear to be homogeneous, both regarding velocity and thickness, except in the vicinity of the kimberlite field. This heterogeneous upper crust may reflect the structure inherited from the processes of Proterozoic amalgamation of terranes and microcontinents in the area, which may mainly have affected the upper parts of the crust. However, it appears more likely that later secular, metamorphic processes have equilibrated the amalgamated lower and middle crust laterally, and removed most of the original lateral differences in velocity structure. Crustal, seismic normal-incidence reflection sections from Precambrian cratons often show distinct signs of original structure from the formation and amalgamation of the crust, e.g. a reflection fabric that may be interpreted as images of anastomosing, ductile shear zones (Abramovitz et al., 1997) or reflective zones that indicate original compressional tectonic shear zones (e.g. (BABEL Working Group, 1993). Such structure has probably been preserved during the period since the Proterozoic, while metamorphic or other processes have modified the crust to a sub-horizontal seismic velocity structure as observed in Yakutia.

Despite the relatively homogeneous appearance of the overall crustal velocity structure along both profiles, there is also distinct variation that may correlate with the contacts between the main tectonic provinces, such as at the transition between the Magan and the Anabar provinces in profile II at km 400. This indicates that differences between the amalgamated terranes and microcontinents still influence the seismic velocities. Likewise, the distinct change in velocity structure at the southern end of profile II into the Nepa-Botuobuya anteclise provides strong evidence for inherited differences in crustal structure.

The velocity model along profile II shows an abrupt uplift of the Moho by 5 km at the transition from the platform into the Vilyui basin. This may indicate thinning of the crust associated with the Devonian stretching event of the Eurasian Platform, which caused the development of a series of aulacogens or rift zones. There is similar indication for crustal thinning at the northern end of profile I where the profile extends into the Predpatom basin.

We interpret a distinct velocity anomaly with a lower to normal velocity centre inside a 120-km wide rim of elevated velocity to >6.3 km/s in the central part of profile I. The low-velocity anomaly disrupts the continuity of the seismic interface between the upper and the middle crustal layers and it extends to the top of the lower crust at a depth of ca 25 km. Its projection to the Moho coincides with the location of a 70-km wide zone of small mantle velocity, although there is no corresponding anomaly in the lower crustal velocity. This anomaly probably is related to the presence of the kimberlite field, although the anomaly is slightly displaced northward by ca. 20 km from Mirnyi at the surface. We speculate that the elevated velocity may be caused by the presence of magmatic rocks in the uppermost crust or that metamorphic processes induced by the heat from the intruded kimberlite pipes may have altered the crustal rocks within a distance of 60 km. The relatively small velocity (or normal velocity inside elevated velocities?) in the centre of the anomaly may be caused by fracturing by the intrusion of the kimberlite pipes together with alterations due to the abrupt heating and subsequent cooling.

The lower crustal velocities appear non-disturbed by the presence of the kimberlite. However, the top of the lower crustal layer is uplifted by ca. 5 km in a 180-km wide interval in the central part of profile I, and this uplifted area extends into the Viluyi basin along profile 2. The sequence between the emplacement of the kimberlite and the basin is unknown. Hence, it is possible that the kimberlite intruded into the crust before the formation of the Viluyi basin or rift. If the thickened lower crust around the Vilyui basin is caused by underplating related to the rifting processes, we should expect that any anomaly in the lower crust from the emplacement of the kimberlite have been destroyed by the rifting.

Extremely large velocity of 8.7 km/s is interpreted in the sub-Moho mantle along most of profile I, with the exception of a 70-km wide anomaly with “normal” velocity of around 8.1 km/s. The major part of the crossing profile II has an upper mantle velocity of around 8.2 km/s with two 55–80-km wide zones with very large seismic velocity of at least 8.5 km/s. Similar extreme velocity has earlier been proposed by Suvorov et al. (1999). Also seismic data recorded from “Peaceful Nuclear Explosions” indicate the existence of very large velocity in this region to depths of around 80–100 km (Egorkin et al., 1987; Pavlenkova, 1996; Nielsen et al.,

1999). It is tempting to explain the large velocity by >4% anisotropy. However, areal seismic surveys of Pn velocity in Yakutia indicate that there is no preferred direction of the large velocity (Suvorov et al., 1999). These latter surveys used areal coverage of the region with seismic stations and shots with a good azimuthal coverage of Pn propagation directions. However, the coarse sampling prevents unique interpretation. Also, the PNE studies indicate that the large velocities are measured in two perpendicular directions over much of the Yakutian kimberlite region. The evidence presented here certainly indicates that anisotropy may play a role, although the evidence is not conclusive. Anisotropy of mantle rocks is often explained by alignment of olivine crystals, which may cause anisotropy factors up to 20% in extreme cases (Kern, 1993; Kern and Tubia, 1993; Christensen, 1996). The abrupt terminations of the zones of extremely large velocity and their presence in both profiles make it possible that the gross sampling of the Pn velocity by the areal surveys may have prevented identification of anisotropy and that the tendency toward determination of average velocity has masked for the variation, which has relatively short wavelength.

The abrupt termination of the zones of large velocity also presents a problem for interpretation of the extreme velocities in terms of anisotropy. It appears difficult to explain how different, strongly anisotropic mantle zones may be brought into direct contact with transition widths of less than 20 km, unless the anisotropic zones already existed at the time of the original amalgamation of the provinces, such that they were brought together by tectonic processes.

It appears that the extremely large velocity may be characteristic for kimberlite provinces, perhaps even for diamond bearing kimberlite provinces. Such large velocity has, so far, been identified in Yakutia and in the Trans-Hudson Orogenic area in Canada, which includes one diamond-bearing kimberlite field (Nemeth and Hajnal, 1998). One may speculate that the anisotropic mantle material may have influenced the intrusion of the kimberlite pipes. The results from Canada also indicate that the sub-Moho mantle may consist of anisotropic rocks with measured variation in two perpendicular directions between 8.3 and 8.6 km/s. The fast axis appears to be dominantly north–south directed, in agreement with the finding of a fast SKS polarization direction of 34–42° (Ellis et al., 1996). The refraction results from Canada also indicate abrupt terminations of the zones with extremely large velocity, possibly coinciding with main tectonic borders (Nemeth et al., 1996).

If the main cause of the extremely large velocities is not anisotropy, it should be in terms of isotropic bulk properties. Whereas seismic velocities of 8.7 km/s have often been measured in anisotropic rock (e.g. Kern, 1993; Kern and Tubia, 1993), there exists to our knowledge no laboratory measurements of such high isotropic velocity on samples. An isotropic velocity of 8.7 km/s at a depth of ca. 50 km requires abnormal mineralogy, despite the very small temperatures in the Yakutian mantle. Samples of large garnet minerals are often observed in the area (Pokhilenko, personal information). If garnet might exist in large quantity in the sub-Moho mantle in Yakutia, this would definitely explain the measured extremely large velocities. However, the required amount of garnet or similar high-velocity minerals would be huge. To explain the observation of strong Pn phases, one would require that the layer with the large velocities extends at least over a depth interval comparable to the seismic wavelength. This is of the order of 1.5 km at the main frequency of 6 Hz for the observed Pn phases. Therefore, a garnet-rich layer with a thickness of around 2 km would be required over a large part of the Yakutian kimberlite province if such mineralogy should explain the observation. The similar observation in the PNE data would indicate the need for an even thicker layer due to the lower frequency content of such data. We have not found any compelling difference in the amplitude variation and critical offset of the PmP reflection from the Moho that could indicate whether the velocity difference across the Moho is related to anisotropy. Further measurements are needed to resolve the issue of anisotropy or isotropy as the cause of the extremely large seismic velocities that we observe around the Mirnyi kimberlite field. We have only access to measurements along two crossing profiles, which have been sampled relatively coarsely laterally. We find that additional seismic profiling along profiles as well as by areal coverage with dense sampling is necessary for obtaining compelling data to resolve the question of anisotropy at Mirnyi.

9. Conclusions

We have presented the results from interpretation and modelling of newly digitized seismic data that have been digitized from analogue DSS data, which was acquired in 1981 and 1983 along two profiles of total length about 710 km. The reinterpretation was carried out by application of ray tracing modelling of the seismic data in two dimensions for a regional seismic velocity model of the crust and uppermost mantle

around the Mirnyi kimberlite field. On the basis of our interpretation, we may conclude:

1. Extremely large seismic Pn velocity of 8.7 km/s has been measured along most of one profile and of ~8.5 km/s along parts of a crossing profile around the Mirnyi kimberlite field. Such large velocities may be explained by anisotropy of the mantle rocks, but we cannot exclude the possibility that they are caused by isotropic rock properties, which, however, are difficult to justify from current laboratory measurements.
2. The crustal thickness is 40–45 km with generally only smooth variation, except at the transition between the Siberian platform and the Vilyui rift.
3. The crustal architecture consists of three main layers similar to other cratonic areas. The velocities of the three main layers are 6.0–6.3, 6.4–6.5 and 6.8–6.9 km/s.
4. The upper crustal layer has strong lateral variation in velocity between 6.1 and 6.5–6.6 km/s. A clear anomaly is observed at the kimberlite field, extending to a depth of 25 km.

References

Abramovitz, T., Berthelsen, A., Thybo, H., 1997. Proterozoic sutures and terranes in the southeastern Baltic Shield interpreted from BABEL deep seismic data. Tectonophysics 270, 259–277.

Artemieva, I.M., Mooney, W.D., 2001. Thermal structure and evolution of Precambrian lithosphere: a global study. Journal of Geophysical Research 106, 16387–16414.

BABEL Working Group, 1993. Deep seismic reflection/refraction interpretation of the crustal structure along BABEL profiles A and B in the southern Baltic Sea. Geophysical Journal International 112, 325–343.

Boyd, F.R., Gurney, J.J., 1986. Diamonds and the African lithosphere. Science 232, 472–477.

Brachvogel, F.F., 1984. Geological aspects of kimberlite magmatism on the northeast of the Siberian platform. Yakutsk: Siberian Branch of Academy of Sciences of USSSR, Yakutsk. 128 pp.

Christensen, N.I., 1996. Poisson's ratio and crustal seismology. Journal of Geophysical Research B, Solid Earth and Planets 101, 3139–3156.

Duchkov, A.D., Sokolova, L.S., 1997. Thermal structure of the lithosphere of the Siberian platform. Russian Geology and Geophysics 38, 528–537.

Duhovskyi, A.A., Artamonova, N.A., Dudko, E.A., 1986. Deep structure of kimberlite field of Siberian platform (in Russian) Reports of Academy of Sciences of USSR 290, 920–924.

Egorkin, A.V., Zuganov, S.K., Pavlenkova, N.A., Chernyshev, N.M., 1987. Results of lithospheric studies from long-range profiles in Siberia. Tectonophysics 140, 29–47.

Ellis, R.M., Hajnal, Z., Bostock, M.G., 1996. Seismic studies on the Trans-Hudson Orogen of western Canada. Tectonophysics 262, 35–50.

Erinchek, Y.M., Erkhov, V.A., Parasotka, B.S., 1994. Prospecting for primary diamond deposits by geophysical methods. Proceedings of the Second International Symposium "Mineral Resources of Russia" St. Petersburg 24–31.

Griffin, W.L., et al., 1999. The Siberian lithosphere traverse: mantle tarranes and the assembly of the Siberian craton. Tectonophysics 319, 1–35.

Grinson, A.S., 1997. A model of kimberlite formation from geology–geophysical data. Geofizika 6, 17–32 (in Russian).

Groves, D.I., Ho, S.E., Rock, M.S., Barley, M.E., Muggeridge, M.T., 1987. Archean cratons, diamond and platinum; evidence for coupled long-lived crust–mantle systems. Geology 15 (9), 801–805.

Haggerty, S.E., 1986. Diamond genesis in multiply constrained mantle. Nature 320, 34–38.

Karaev, N.A., Biezais, Y.Y., Lebedkin, P.A., 2000. Seismic heterogeneity of kimberlite-forming systems. Geofizika 6, 17–32 (in Russian).

Kern, H., 1993. P- and S-wave anisotropy and shear-wave splitting at pressure and temperature in possible mantle rocks and their relation to the rock fabric. Physics of The Earth and Planetary Interiors 78, 245–256.

Kern, H., Tubia, T.B., 1993. Pressure and temperature dependence of P- and S-wave velocities, seismic anisotropy and density of sheared rocks from the Sierra Alpujata massif (Ronda peridotites, southern Spain). Earth and Planetary Science Letters 119, 191–205.

Manakov, A.V., Romanov, N.N., Poltoratckaya, O.L., 2000. Kimberlite fields of Yakutia. Issue of Voroneg State University 82.

Meissner, R., 1986. The continental crust: a geophysical approach. International Geophysics Series, vol. 34. Academic Press, New York.

Nemeth, B., Hajnal, Z., 1998. Structure of the lithospheric mantle beneath the Trans-Hudson Orogen, Canada. In: Klemperer Simon, L., Mooney Walter, D. (Eds.), Deep Seismic Profiling of the Continents: II. A Global Survey. Tectonophysics. Elsevier, Amsterdam, Netherlands, pp. 93–104.

Nemeth, B., Hajnal, Z., Lucas, S.B., 1996. Moho signature from wide-angle reflections; preliminary results of the 1993 Trans-Hudson Orogen refraction experiment. Tectonophysics 264, 111–121.

Nielsen, L., Thybo, H., 2003. The origin of teleseismic Pn waves: multiple crustal scattering of upper mantle whispering gallery phases. Journal of Geophysical Research 108, 2460. doi:10.1029/2003JB002487.

Nielsen, L., Thybo, H., Solodilov, L., 1999. Seismic tomographic inversion of Russian PNE data along profile Kraton. Geophysical Research Letters 26, 3413–3416.

Pavlenkova, N.I., 1996. General features of the uppermost mantle stratification from long-range seismic profiles. Tectonophysics 264, 261–278.

Pokhilenko, N.P., Sobolev, N.V., Kuligin, S.S., Shimizu, N., 1999. Peculiarities of distribution of piroxenite paragenesis garnets in Yakutian kimberlites and some aspects of the evolution of the Siberian Craton lithospheric mantle. 7th Intern. Kimberlite Conf. P. H. Nixon vol., Cape Town, pp. 689–698.

Priestley, K., Debayle, E., 2003. Seismic evidence for a moderately thick lithosphere beneath the Siberian platform. Geophysical Research Letters 30, 1118–1121.

Rosen, O.M., Kent, C., Natapov, L.M., Nozhkin, F.D., 1994. Archean and early Proterozoic evolution of the Siberian craton: a preliminary assessment. In: Condie, K. (Ed.), Archean Crustal Evolution. Elsevier, Amsterdam, pp. 411–459.

Safronov, A.F., Suvorov, V.D., Zaitcev, A.I., 1990. Kimberlite magmatizm markers in the crust and uppermost mantle of the South-West of Yakutia. Reports of Academy of Sciences of USSR 312 (7), 12–17.

Safronov, A.F., Smelov, A.P., Zaitcev, A.I., 2001. Problems of tectonic control of diamond-bearing kimberlites in the Siberian Platform. Otechestvennaya Geologia 5, 3–5.

Sandmeier, K.J., Wenzel, F., 1990. Lower crustal petrology from wide-angle P- and S-wave measurements in the Black Forest. Tectonophysics 173, 495–505.

Sobolev, N.V., 1974. The deep-seated inclusions in kimberlites and the problem of the upper mantle composition. Nauka, Novosibirsk, Siberian Branch (In Russian), 204.

Sobolev, V.S., Sobolev, N.V., 1971. The nature of the Mohorovichich boundary and mineral composition of upper mantle from petrography data. In: Davydova, N.I., Resanov, I.A. (Eds.), Nature of Seismic Boundaries in the Crust. Nauka, Moscow, pp. 112–116.

Suvorov, V.D., Kreinin, A.B., Seleznev, V.S., Soloviev, V.M., V.F.U., 1983. Deep seismic studies along a profile of the Olguidakh river–Lensk town. Geologia and Geophizika 9, 72–80 (in Russian).

Suvorov, V.D., et al., 1986. Deep seismic study along profile Tas-Urach–Malykai villages. Geologia and Geophizika 11, 72–78 (in Russian).

Suvorov, V.D., Timirshin, K.V., Yurin, Y.A., Parasotka, B.S., Matveev, V.D., 1997. Ratio of deep-seated and near-surface structures in southern part of Yakutian kimberlite province according to seismic data. Russian Geology and Geophysics 38 (5), 1054–1061.

Suvorov, V.D., Parasotka, B.S., Chernyi, S.D., 1999. Deep seismic sounding studies in Yakutia (Translated from Fizika Zemli, Nos. 7–8, pp. 94–113). Izvestiya Physics of the Solid Earth 35 (7–8), 612–629.

Thybo, H., Luetgert, J., 1990. RAY84PC—two-dimensional ray tracing and synthetic seismogram calculation on personal computers. Open File Report. Institute of Geology, Copenhagen, pp. 1–4.

Thybo, H., Perchuc, E., Gregersen, S., 1998. Interpretation in statu nascendi of seismic wide-angle reflections based on EUGENO-S data. Tectonophysics 289 (4), 281–294.

Thybo, H., et al., 2003. Upper lithospheric seismic velocity structure across the Pripyat Trough and the Ukrainian Shield along the EUROBRIDGE'97 profile. Tectonophysics 371, 41–79.

Uarov, V.F., 1981. Seismic distinctive features of the upper mantle in western Yakutia. Geologia and Geophisika 9, 120–124 (in Russian).

Vaganov, V.I., et al., 1995. Forecast-exploration systems for diamond deposits. Otechestvennaya Geologia 3, 42–53 (in Russian).

Zhang, Y.-S., Tanimoto, T., 1993. High-resolution global upper mantle structure and plate tectonics. Journal of Geophysical Research 98 (6), 9793–9823.

Zonenshain, L.P., Kuznin, M.I., Natapov, L.M., 1990. Tectonics of the lithospheric plates of the USSR territory. Nedra 325, 330.